2021

Material Analysis of 3D Welded 5356 Aluminum Alloy

Ryan Fouts
South Dakota State University

MATERIAL ANALYSIS OF 3D WELDED 5356 ALUMINUM ALLOY

BY

RYAN FOUTS

A thesis submitted in partial fulfillment of the requirements for the

Master of Science

Major in Mechanical Engineering

South Dakota State University

2021

THESIS ACCEPTANCE PAGE

Ryan Fouts

This thesis is approved as a creditable and independent investigation by a candidate for the master's degree and is acceptable for meeting the thesis requirements for this degree. Acceptance of this does not imply that the conclusions reached by the candidate are necessarily the conclusions of the major department.

Todd Letcher
Advisor Date

Kurt Bassett
Department Head Date

Nicole Lounsbery, PhD
Director, Graduate School Date

This thesis is dedicated to my

family for their love and sacrifice.

ACKNOWLEDGEMENTS

There have been many people who have had a hand in this, probably more than I can name. Here are some people I would like to thank and acknowledge:

I would like to thank my advisor, Dr. Todd Letcher, for his guidance, trust, and support which was instrumental in the completion of this thesis. He gave me a start in the 3D print lab and led to this moment. Dr. Letcher has been a great mentor and role model. This would not have been possible without his help.

I would like to thank my amazing and beautiful wife, Emma, for her love, support, and sacrifice. Her loyalty, encouragement, and perseverance has kept me motivated to succeed. I cannot thank her enough for her sacrifice during the past few years.

My thesis committee members, Dr. Anamika Prasad and Dr. Peter Troy White, for their valuable time and feedback. Additionally, Dr. Prasad, for her expertise and guidance.

My parents, Kevin and Lisa Fouts, for their love, support, and encouragement. Their countless sacrifices have provided the opportunity to reach this point in my college career.

Dr. Jeffrey Doom for his encouragement and support.

Gary Hatfield for his assistance and guidance with statistical analysis of data.

Shop supervisors, Tyler Hanks and Garrett Walter, for their time, knowledge, and willingness to help.

My senior design group members, John Bachman, Matt Fitzgerald, Madelynn Hotchkiss, Scott Landes, and Ethan Steiner, for helping get this project started. I appreciate their time and efforts to make this possible.

Cory Jacques for helping prepare samples, staying late in the shop, and encouragement.

Dylan Dulas, Brock, Tom, and Dante, who have worked on the printer in a variety of capacities.

I would like to thank my classmates, professors, friends, and family for being there for me when I needed it.

Finally, above all, I would like to thank God for his grace, filling my life with these people, and giving me my abilities.

CONTENTS

ABBREVIATIONS

AM	Additive manufacturing
AZ	Arc Zone
CAD	Computer-Aided Design
cfh	cubic feet per hour
CMT	Cold Metal Transfer
CMT-P	Cold Metal Transfer Pulsed
CNC	Computer Numerical Control
DC	Direct Current
DED	Direct Energy Deposition
DMLS	Direct Metal Laser Sintering
FDM	Fused Deposition Modeling
FFF	Fused Filament Fabrication
g	gram
GMAW	Gas Metal Arc Welding
HAZ	Heat Affected Zone
lb	pound
LZ	Light Zone
MIG	Metal Inert Gas
mL	milliliter
mm	millimeter
Pa	Pascal
PBF	Powder Bed Fusion
s	second
SEM	Scanning Electron Microscope

SLA	stereolithographic apparatus
SLS	selective laser sintering
std dev	standard deviation
UV	Ultraviolet
WAAM	Wire Arc Additive Manufacturing
XRD	X-ray Diffraction
σ	stress
ε	strain

LIST OF FIGURES

LIST OF TABLES

ABSTRACT

MATERIAL ANALYSIS OF 3D WELDED 5356 ALUMINUM ALLOY

RYAN FOUTS

2021

Metal 3D printing has been reserved for aerospace and high-end automotive industries because of its cost. A gas metal arc welder (GMAW) on a rugged 3D printer frame could make metal additive manufacturing an option for more industries and consumers. 3D welded aluminum has not been examined in depth as an option for additive manufacturing (AM). Extensive tests are necessary to determine the correct settings to use a metal inert gas (MIG) welder for AM. Porosity within the welded material must be evaluated to better understand the additive process. The material properties of 3D welded aluminum will be tested and compared to existing additive and traditional manufacturing methods. If strong enough this could reduce the cost of aerospace expeditions making tools like CubeSats more accessible to lower budget entities. Additionally, metal additive manufacturing could become more available and cost effective to use in any industry that requires manufacturing.

INTRODUCTION

Additive manufacturing (AM) and 3D printing is a modern method of manufacturing where, as the name implies, material is added until the desired final form is reached. To achieve this, a CAD model is sliced into layers and toolpaths allowing the machine to deposit material appropriately. G-code is generated from the sliced model to communicate with and control the printer by moving the printer along its axes. 3D printers usually have three axes of motion – x, y, and z – which allow for three dimensional controls. A controller with a 3D print firmware is used to interpret the g-code and rotates motors to obtain the desired toolpaths. Motion is obtained by translating the rotational motion of motors to linear motion using belts, screws, and rack and pinions.

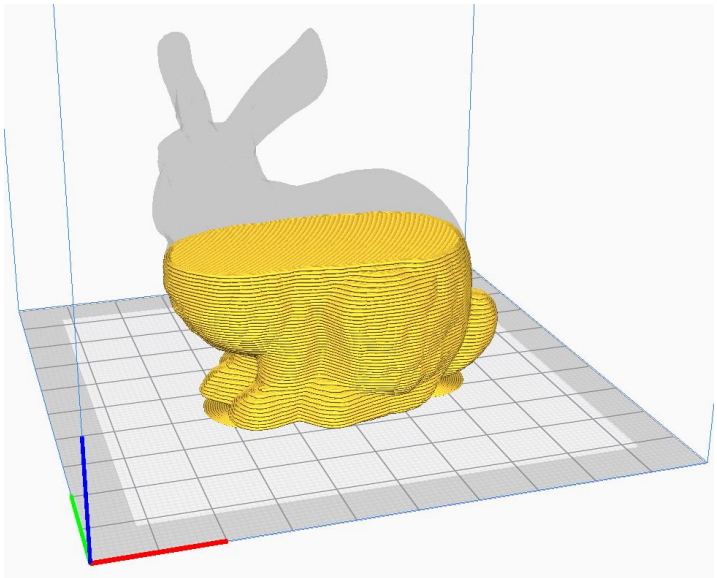

Figure 1. Model sliced with a coordinate system [1].

The history of 3D printing began in the 1940's with the creation of CNC machines. CNC technologies were originally used to precisely control milling machines which use a similar x, y, z coordinate system to modern 3D printers. The first documented 3D printer was a stereolithographic (SLA) printer where layers of liquid are

solidified by UV light. A bed moves and the light can harden the next layer of material to the previous. The result was autonomous, rapid creation of parts with complex geometries that are not attainable with traditional manufacturing methods. Hence, the name rapid prototyping. In 1988, the first selective laser sintering (SLS) printer was produced, which used a laser to sinter, or partially melt, a layer of powder material together. The bed is lowered more powder is added and the laser sinters the powder to the previous layer. Fused deposition modeling (FDM), currently the most recognized type of 3D printing, was created in 1989. FDM heats a plastic filament which is forced through a nozzle creating lines of melted filament that cool in layers [2][3][4].

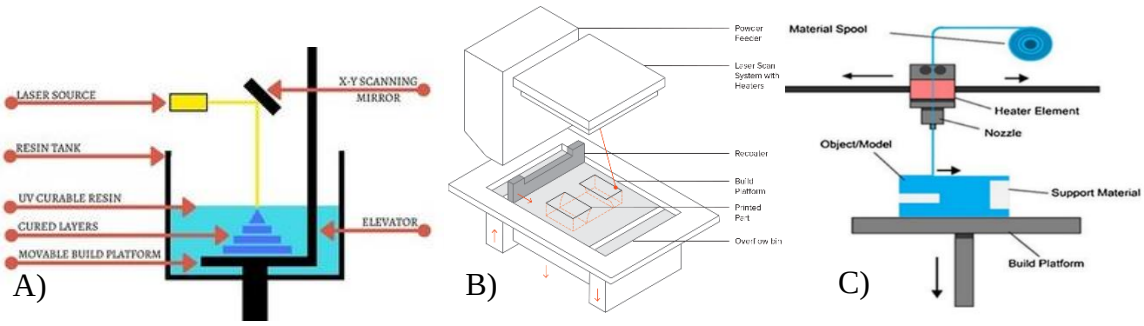

Figure 2. A), B), & C) Schematics of an SLA, SLS, and FDM printers, respectively [5][6][7].

Additive manufacturing offers some benefits over traditional manufacturing - machining (subtractive), casting, molding, forming, coating, and joining [8][9]. Comparable manufacturing methods to 3D printing are casting, molding, and machining because they can create parts with a variety of geometries. 3D printing allows for producing parts with highly complex and precise geometry that traditional methods are not capable of. The process of 3D printing is inherently less wasteful because the material is placed only where it is needed, whereas in traditional manufacturing processes extra material is ground or machined away – casting and molding being the exception. Waste

material from 3D printing can be recycled to be printed again and less energy is required to make parts. When compared to molding, 3D printing is more environmentally friendly [10]. Depending on the part being made, additive manufacturing can produce parts quicker than traditional methods [11]. Additive manufacturing is also decreasing costs of prototyping and final production [12]. A variety of materials are capable of being 3D printed whereas some traditional methods are limited in their capabilities. Additive manufacturing allows for less parts in the assembly, less material waste, and faster production of a final product. Depending on the part, additive manufacturing can produce a prototype much quicker than traditional methods, explaining why 3D printing and rapid prototyping have become synonymous.

In its early stages, 3D printing was primarily used for prototyping purposes and almost exclusively used polymers as building materials. Recently, more materials have been used in additive manufacturing allowing for use in industry. Printer filament is made of a variety of polymers allowing for different characteristics. Some filament contains wood, carbon fiber, or metal powders [13]. Entire buildings have been printed by schools and teams, including the Army Corps of Engineers, with the goal of being able to autonomously create dwellings. This means that structures can be built with little to no human interaction keeping people safe and reducing building costs [14]. Advancements in printing methods allows for using biological materials for medical applications. Technology for 3D printed organs is being researched to decrease the probability of rejection. 3D printing small organs using a patient’s stem cells is being researched to reduce chances of rejection. Prosthetics are made quicker and to increase the patient’s quality of life. Joint replacements are another way additive manufacturing is being used

in the medical field to improve the lives of patients [15][16]. Metal 3D printing is beginning to change the way aerospace, automotive, and manufacturing industries operate. Aerospace companies have been testing rocket engines and fuel tanks that have been 3D printed [17]. Turbine blades for jet engines have been researched and tested by different companies [18][19]. The automotive industry has been using additive manufacturing for creating performance intakes with complex geometries, and Local Motors 3D printed the body of a car [20][21].

Metal additive manufacturing is a category of 3D printing on its own with different methods of metal 3D printing in existence. Most metal 3D printing is produced for large companies because of the high cost. Powder bed fusion (PBF) and direct energy deposition (DED) are the two main types of metal additive manufacturing and are beginning to become more widely used in industry for specialized tasks. PBF is similar to SLS as it starts with a bed of powder, in this case metal instead of plastic powder, and a powerful laser or electron beam melts or sinters the metal powder. After the layer is complete, more powder is swept over the bed and the process repeats until the part is complete. A schematic of a PBF printer is shown in figure 3. DED encompasses a wide range of metal 3D printers. DED printers use one or more energy sources to melt material as it is added to the part. The energy sources used in DED are electric arc, electron beam, and high-power laser, while feedstock can be in the form powder or wire. Generally, the powder feedstock for DED is larger than that of PBF [22]. Schematics of such printers are shown in figure 3.

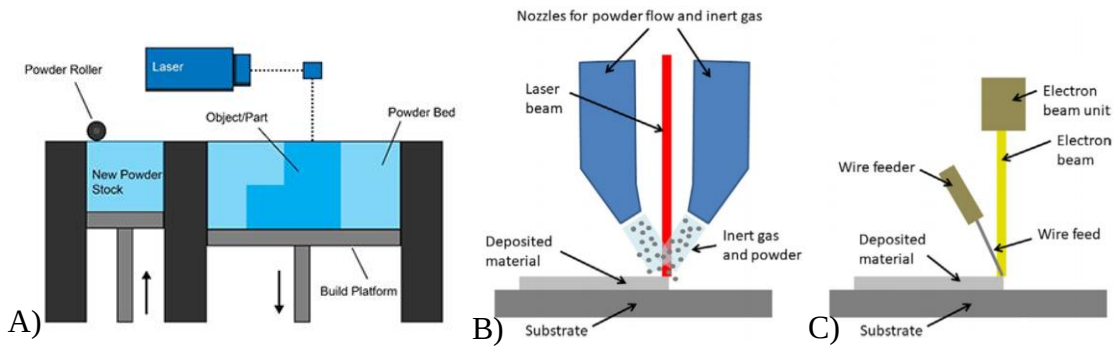

Figure 3. A) PBF printer schematic [23]. B) DED using a laser energy source and powder feedstock. C) DED using an electron beam energy source and wire feedstock [24].

Binder jetting and sheet lamination are metal AM methods that are not as common, and research/publications are scarce. The process of binder jetting is when a binding agent is added to a powder bed in a controlled manner then curing it. This step is like an SLS printer but with a glue instead of a sintering process. Once complete, the part is sintered to make the metal one piece. Sheet lamination as the name implies is when thin sheets of metal are added layer by layer, usually through some type of metal bonding process like brazing or welding. As sheets are added, the layers begin to create a 3D shape [24]. A newer type of metal printing is joule printing. The process is like DED but uses resistance to melt the material instead of an arc, laser, or electron beam. A joule printer is fast and acts like a metal version of an FDM printer [25][26].

There are a variety of metal AM methods in use because there is no correct way to AM metal. Some processes have benefits like faster print speed, tighter tolerances, larger print volume, or low cost to own and operate. Some of the cheapest commercially available metal 3D printers are available for around $100,000 [27]. Initial cost is only a fraction of the overall price and the cost to run the printer (power and feedstock) must be factored in. The price of powdered metal for additive manufacturing can range from $80-600/kg depending on the metal [28]. Aluminum welding wire can be $8-15/lb, or about

$17-33/kg, and is readily available through any welding supplier [29]. Digital Alloys also states that titanium powder can cost $100-500/kg versus titanium wire costing $125-175/kg [30]. The deposition rate and potential part size is also much faster and larger for wire fed printers as opposed to powder fed. Powder printers have excellent dimensional accuracy and print more complex geometries. In figures 4, 5, & 6. the costs and benefits of each type of printing method are shown.

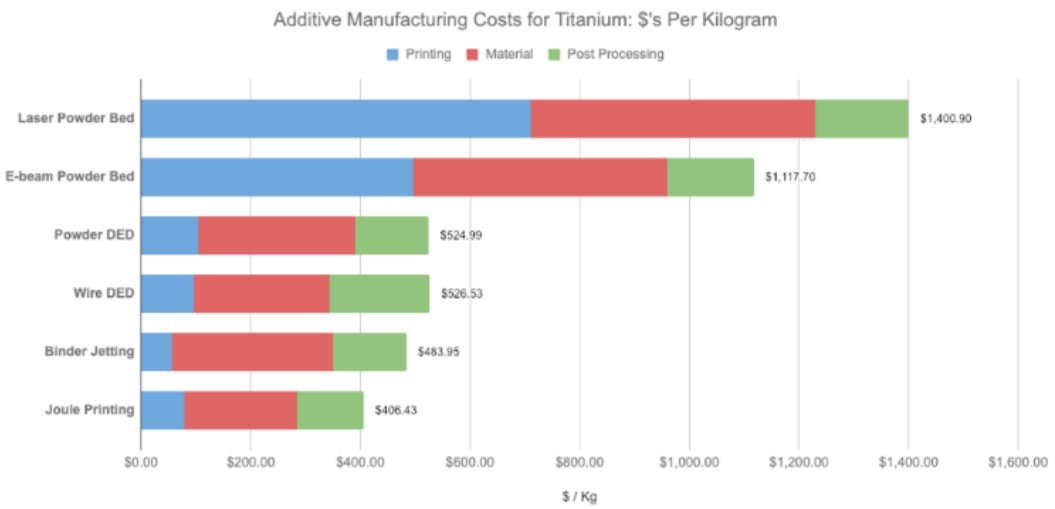

Figure 4. Cost per kg based on different metal printing methods [31].

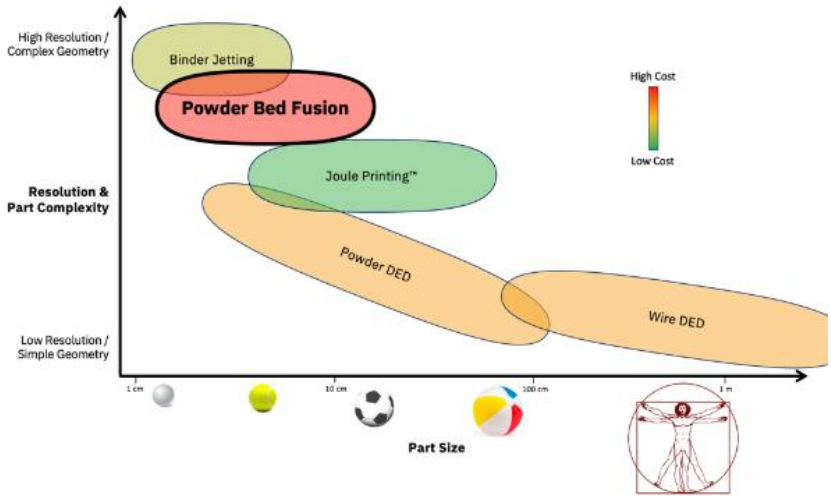

Figure 5. Plot showing printer part size vs resolution & compatibility [32].

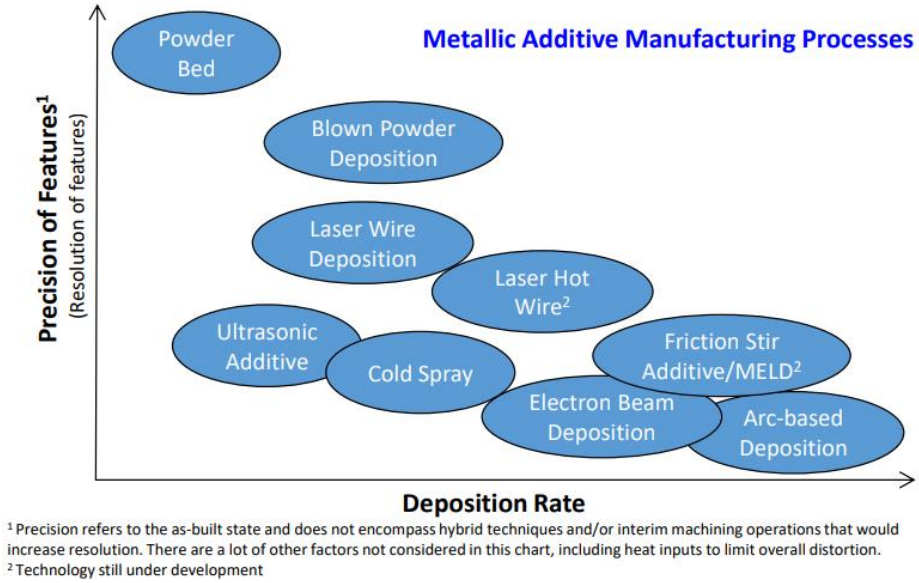

Figure 6. Plot showing deposition rate vs precisions [33].

Currently, some industry leaders in metal additive manufacturing are Stratasys [34], Mark Forged [35], Titomic [37], DMG Mori [38], Gefertec [39], Wolf [40], Relativity [17], Sciaky [42], and MX3D [43]. Stratasys makes parts for using direct metal laser sintering (DMLS), a subset of PBF. Stratasys, DMG Mori, and many others using a similar DMLS/SLS process can make dimensionally accurate parts from stainless steel, aluminum, nickel, titanium, and cobalt [34]. The cheapest DMLS/SLS printers cost $250,000 and do not offer much print volume – about 100mm x 100mm x 100mm [27]. Mark Forged has a printer called Metal X that uses a metal fused filament fabrication (FFF) process. FFF is the same as FDM, but uses a proprietary metal infused filament, requires support material to be washed away, and the part must be sintered to obtain a complete metal part. The benefit of the system is that it can print a variety of materials: stainless steel, tool steel, inconel, and copper [35]. Mark Forged boasts the printer's affordable price of $99,500 [36], while competitors like Desktop Metal offer a similar unit for $60,000 without the furnace [27]. These processes are innovative and useful, but

the parts may need more research to ensure use in production parts. Titomic, a parts manufacturer, creates large parts using a combination of cold spray additive and subtractive manufacturing. Cold spray is when hot gases and metal particles are forced and concentrated by a spray gun at a high velocity on a point. The collision of the particle on the material creates a bond. Titomic boasts a 9m x 3m x 1.5m build volume using 3-axis motion in conjunction with a 5-axis robotic arm and can create parts out of titanium, steel, copper, nickel, and magnesium. Titomic also makes a smaller unit that has a build volume of 1m x 1m x 1m [37].

DGI Mori, Gefertec, and Wolf Robotics (a Lincoln Welding brand) all make DED printers with a variety of sizes, capabilities, and capacities. DMG makes powder bed and laser DED printers with powder feedstock [38]. Gefertec makes large arc wire fed printers that also use mills for better dimensional accuracy. The welding and milling volume of Gefertec's largest machine is $3m^3$ [39]. Wolf uses large robotic welders capable of additive manufacturing and has produced parts for a small excavator. The least expensive of all these options is still $100,000 and will only produce steel and/or aluminum [40]. MX3D and Relativity Space have produced DED printers capable of large-scale prints. Relativity uses an arc with wire feedstock and a closed loop feedback to produce large parts like a rocket fuel tank. The company also has DMLS printers and plans to be able to produce an entire rocket in just 60 days using one hundredth the number of parts a standard rocket requires [17][41]. Sciaky has an electron beam additive manufacturing (EBAM) method that uses wire feed and an electron beam to add material. The process is fine-tuned with closed feedback and is capable of printing with a variety of materials that other metal printers cannot [42]. MX3D's printer is wire arc additive

manufacturing (WAAM) in concert with a robotic arm for motion. The printer is capable of manufacturing large scale projects, a pedestrian bridge for example, out of stainless steel [43]. Both MX3D and Relativity use their printers to produce parts, their processes are closely guarded secrets, and their 3D printers are not for sale. Existing metal manufacturing methods are not cheap and cheaper methods have limitations like size, accuracy, or material.

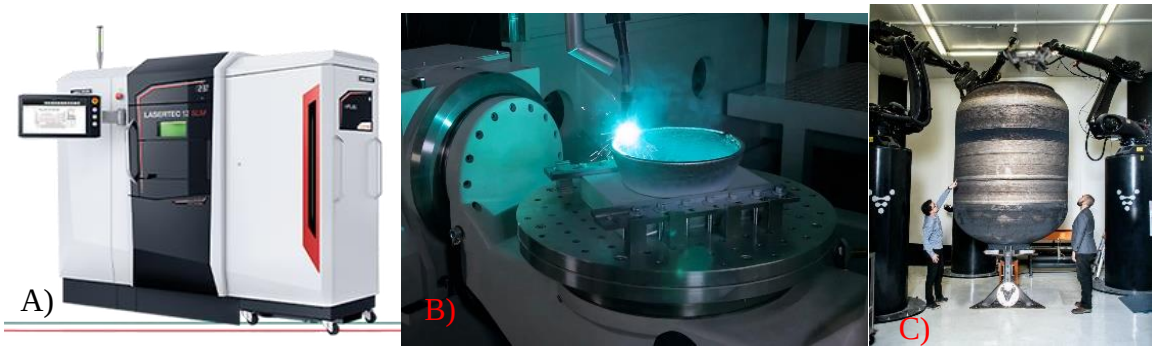

Figure 7. A) A DMG Mori powder bed printer which represents what most DMLS printers look like [38]. B) Inside a Gefertec hybrid printer during the printing process [39]. C) Relativity Spaces large scale printer with completed fuel tank [44].

Several universities are also researching better methods of metal additive manufacturing. For example, Cranfield University has produced a 3D printer using a cold metal transfer (CMT) welder. CMT is a subset of GMAW dip transfer occurs and creates good welds with little splatter and low heat input. Experiments were done with cold metal transfer pulsed (CMT-P) where a spray and dip transfer occur and cold rolling after each weld was performed to improve and refine the material [45]. However, CMT welders are costly so few can access this technology. There are records online that mention TU Delft University students using a MIG welder and Prusa printer to build a metal 3D printer [46]. These records are broad and simply state its existence, no further information on the printer exists. Additionally, Waterloo University students created a metal 3D printer mill

hybrid called the “Metal Maker.” No documentation is publicly available about the Metal Maker other than it prints and mills steel [47]. Titanium and stainless steel manufactured by WAAM have been determined to achieve desirable mechanical properties for use in production parts [48]. Michigan Technological University built an open-source metal 3D printer capable of printing steel and aluminum and has published several papers on advancements upon their printer [49][50][51][52][53][54][55]. The initial paper discusses how the printer was made using a welder and a delta style printer all for under $1,200 [49]. This is a huge leap in progress for metal 3D printing and could make it possible for more people to have access to metal AM. This printer is almost a hundredth the cost of a professional grade metal 3D printer and is without a doubt the most affordable open-source option. MTU developed an open-source voltage and current monitor and arc analyzer for the welding printer and open-source slicer software for metal printing [50][51]. MTU produced documentation on how to turn an existing CNC into a metal printer [52][53]. Two papers on substrate, or print bed material, release has been published by MTU [54][55]. A case study has been done on an excavator arm to determine the validity of large-scale metal additive manufacturing [56].

South Dakota State University researches metal AM with an open source hybrid 3D printer. The goal of the hybrid metal printing project was to produce a metal printer that is cost effective, efficient, precise, and scalable. The budget for the entire printer and supplies was $10,000, when compared to commercially available options this is 10% the cost of the least expensive printers available. The MTU open-source printer is only $1200 [49], however, it has a far smaller build volume and is less capable. The hybrid metal printer will use both a GMAW and milling spindle to obtain rapid and accurate part

production. A similar method is used by 3D Hybrid which has a welding attachment for existing milling machines [57]. The welder will add material to create a rough geometry and the spindle will remove excess material to obtain dimensional accuracy and desired surface finish. This method was chosen because it has relatively low initial and operating cost and has a high deposition rate compared to any other metal manufacturing method [31][32][33]. The hybrid additive manufacturing method is more efficient than traditional manufacturing methods because material is only placed where it is needed, and little material is removed and wasted.

The printer was designed with the aerospace industry in mind. For this reason, aluminum was chosen as the primary feedstock, but the printer is also capable of making parts in steel. Aluminum was chosen despite the difficult welding process because of its strength to weight ratio, corrosion resistance, ease of machining, and conductivity [58][59][60]. The frame and size of the printer targeted a build volume of 1m x 1m x 1m to prove that the 3D aluminum welding method could be used on a large or small scale. The final dimensions of the print volume are approximately 0.5m x 0.65m x 6.5m. To fit a budget or specifications it is possible to build a similar printer using a different scale. The printer outlined here was built to ensure that the process could be proven and reliable with potential for later refinements.

ADAPTABLE HYBRID METAL 3D PRINTER

Many design decisions were made before building the printer. A hybrid system was chosen because the deposition rate, cost, versatility, and availability of materials was better than that of other metal AM methods. The selected welder (Hobart Ironman 230) was chosen because it could weld aluminum and steel, has high duty cycle, and is reasonably priced given the feature set. An economical spindle with enough power to mill aluminum was specified. An x, y, z cartesian printer with a fixed build plate was chosen for the frame of the printer because of its size, capabilities, and complexity. Other options like having a moving plate, delta style motion, and robotic arms were briefly considered, but ruled out because they were not economical or otherwise suited to such a printer.

One concern was that welding and milling can create a harsh environment (weld splatter and metal chips) for regular 3D printer components to function properly. To combat these potential problems, the printer was built robustly with a large steel C channel framework to reduce vibrations from the milling process. In addition to providing stability, this also allows most of the components to be placed in a way that the structure of the printer protected them from the metal chips and weld splatter. Additionally, welding causes material to warp which is why many metal AM printers use a thick build plate. A thick build plate reduces warping, but is very costly. Therefore, thinner ¼ inch 6061 aluminum sheets are used and bolted down to a ½ in steel plate. The steel plate offers rigidity and reduced the cost of multiple large build plates.

Components that were selected for motion of the printer were linear rails, ball screws in the x and y axes, and acme screws in the z axis. Linear rails are well suited for restricting the translation and rotation in undesirable directions and can support large

loads and maintain tight tolerances. This is desirable for the milling process that will cause higher stresses on the frame and potentially misalign the printer. To aid in accurate positional control, ball screws were determined to be the best option. Ball screws offer mechanical advantage which is important during the milling process and convert rotational motion of motors to linear motion needed for control of the printer. Ball screws are used in the x and y axes for fast, accurate, and efficient motion while acme screws are used in the z direction for safety (friction of acme screws are high enough to prevent the print head from dropping in case of power loss).

The welder and spindle need to be able to operate during a print, so one needs to work without interfering with the other. Design options to achieve this were to use a ball screw assembly to move the welder and/or spindle up and down, a tool changing head, and tilting both the welder and spindle into and out of position. A tilting head was designed for the welding torch so that it could be raised out of the way for the milling process to occur. This was deemed the most economical option and is moved by a worm gear box to ensure the assembly would not lower as the milling process was performed. The milling spindle is fixed to the print head to ensure rigid and precise control.

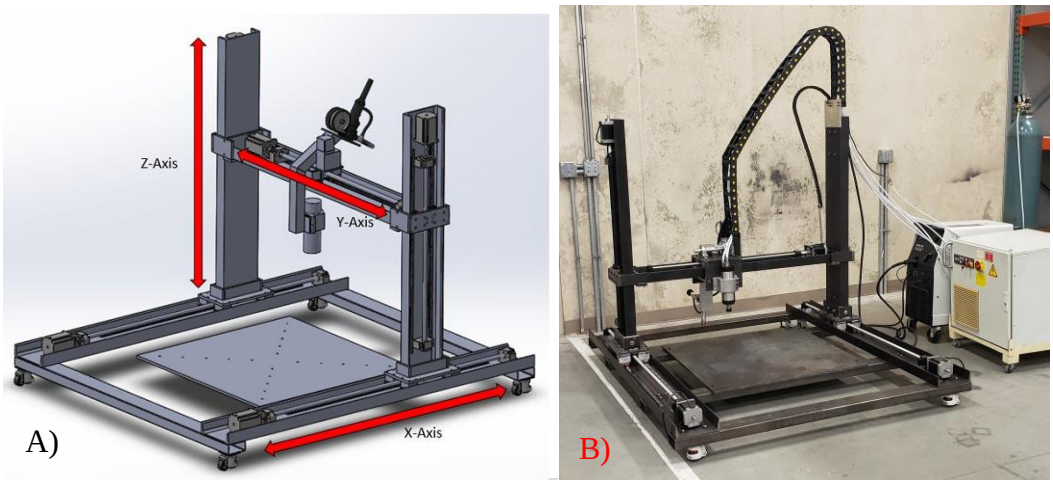

Figure 8. A) Preliminary model in CAD. B) Hybrid GMAW 3D printer setup.

To create motion for the printer, appropriate controls and electronic components must be selected. Stepper motors are typically used to turn the screws and were selected because of their sufficient torque, good accuracy, low cost, and ability to track motion (assuming no skipping). Other options like DC motors, servo motors, and other hybrid motors were considered, but were not as simple to implement or cost effective. Appropriately sized stepper drivers are needed for each of the stepper motors. Steppers are used to control motion in the x, y, and z axes, wire feed, and tilting head. The system uses DC power, so power supplies are chosen based on the required DC voltage. 12 volt and 24 volt (V) power supplies are used to run the stepper motors, extrusion and tilt motors requiring 12V and motors for motion control requiring 24V. It is important to choose a power supply that has enough current to support all the motors being run.

Next, the 3D printer control system is chosen to interpret the G-code commands and produce action from the electrical/mechanical components. Small inexpensive control boards like Raspberry Pi, Arduino, Mach 3, and Duet can be used to run 3D printers. The Arduino Mega was selected because of its ease of use, relatively low price, and existing community support. After the board is wired to the drivers and motors, a firmware must be uploaded to the board to interpret the g-code or software and provide the user interface. There are many open source firmwares available for 3D printing. Initially, Repetier was selected as the firmware because of the easy online configuration tool. Using Repetier did not allow for control of the welder by simply actuating a relay. For this reason, the firmware was switched to Marlin to alleviate this issue despite its slightly more complicated configuration process. Repetier Host is a computer software used to manually control the printer and send g-code to the Arduino controller. G-code

files for the printer are produced using Cura which is an open-source 3D printing software used for many custom or commercially available 3D printers. The addition of weld monitoring hardware like heat sensors or thermal cameras, and a closed feedback loop were considered. This type of a feedback system was determined not possible with the limited budget.

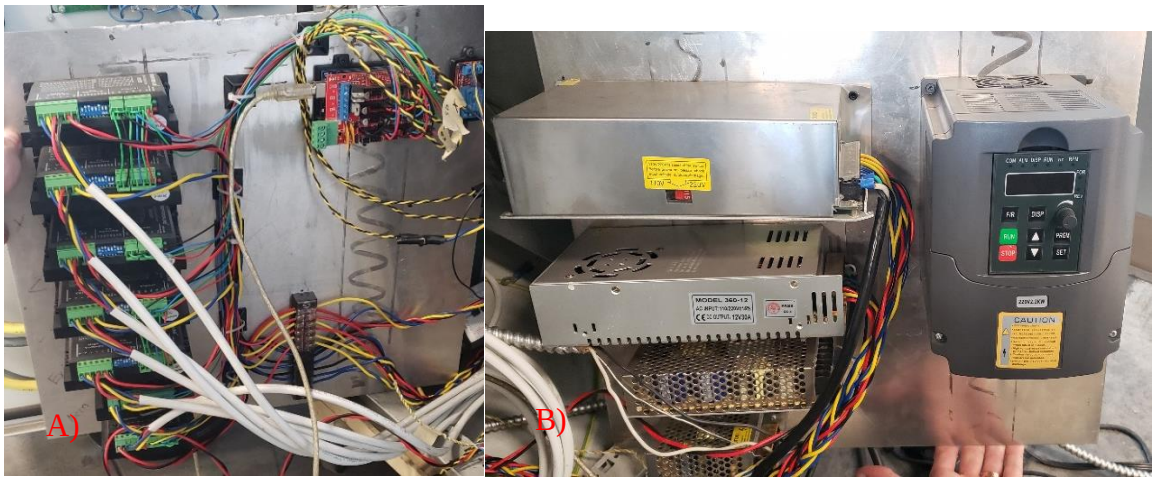

Figure 9. A) Drivers, Arduino, and relay. B) Power supplies and variable frequency drive (VFD) for spindle control.

MATERIAL AND METHODS

To establish appropriate weld parameters, test welds were produced using a variety of settings such as welding voltage/current, wire feed rate, and torch travel speed. The welding wire used in all testing is ER5356. Tables supplied by the manufacturer of the composition and material properties of the welded aluminum wire are shown in tables 1 & 2. ER5356 is a 5000 series aluminum and is an aluminum magnesium alloy with high shear strength and good corrosive resistance [58][59]. Aluminum welding requires a clean surface, so the welding procedure entailed preparing the surface, or substrate, with a wire brush and acetone. After the first weld, and between subsequent welds, the surface was cleaned with a wire brush to remove soot produced by the welding process. Other studies also use cleaning solutions in between welds to try to reduce porosity [61][62]. This is highly idealistic and is not likely to occur during an autonomous print. However, the printer could use the spindle with a wire brush attachment, if necessary, to perform cleaning between layers and maintain an autonomous process. Ideally, the goal would be able to produce parts without the additional step of brushing the surface of the part, but to produce good parts for initial testing, brushing was performed manually between each deposited layer. MTU produced research on substrate release for aluminum welding processes which is good for 3D welded aluminum parts. For this hybrid metal printer, a substrate release is not desirable because during the milling process, the workpiece can experience high milling forces that may remove the part from the build plate. If the workpiece releases from the substrate in the middle of the milling process, this not only causes the part to fail, but it may also cause dangerous conditions for the machine operator.

Table 1. Composition of ER5356 aluminum alloy by percent composition [58].

Si	Fe	Cu	Mn	Mg	Cr	Zn	Ti	Other	Al
0.25	0.4	0.1	0.05-0.20	4.5-5.5	0.05-0.20	0.1	0.06-0.20	0.15	REM

Table 2. Material properties of ER5356 [58].

Melting Range	Conductivity	Density	Anodized Color	Tensile Strength
570-635°C	29% IACS (-0), 27% IACS (-H18)	2657.27 kg/m3	White	38 ksi

For the MIG welding printer, a normal 3D printing slicer cannot be used because the welding process is much different than plastic deposition. Figure 10 shows a severely over penetrated weld using normal FDM printer slicing methods. Over penetration due to concentrated heat means different paths or breaks are needed instead of the normal slicer options. MTU has developed a slicer to help combat this, but was not used in favor of simple and easily quantifiable methods to determine the printer's best settings and produce clean welds [51]. In future work, the slicer will be used to produce parts quickly and automatically.

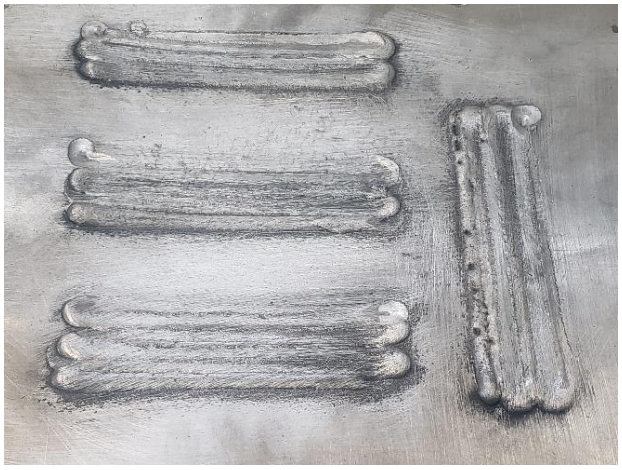

Figure 10. Over penetration due to use of regular 3D printer slicing software.

Since custom G-code files were written to test welding parameters, the DC motor that came in the spool gun was used in conjunction with the welder speed controller and trigger mechanism to avoid having to rewrite many custom G-code files. To convert the arbitrary welder speed settings the desirable unit (mm/s), the wire feed was run at a welder setting for a known time and the length of the wire was divided by the time to approximate the wire speeds in mm/s. The results are shown in the figure below.

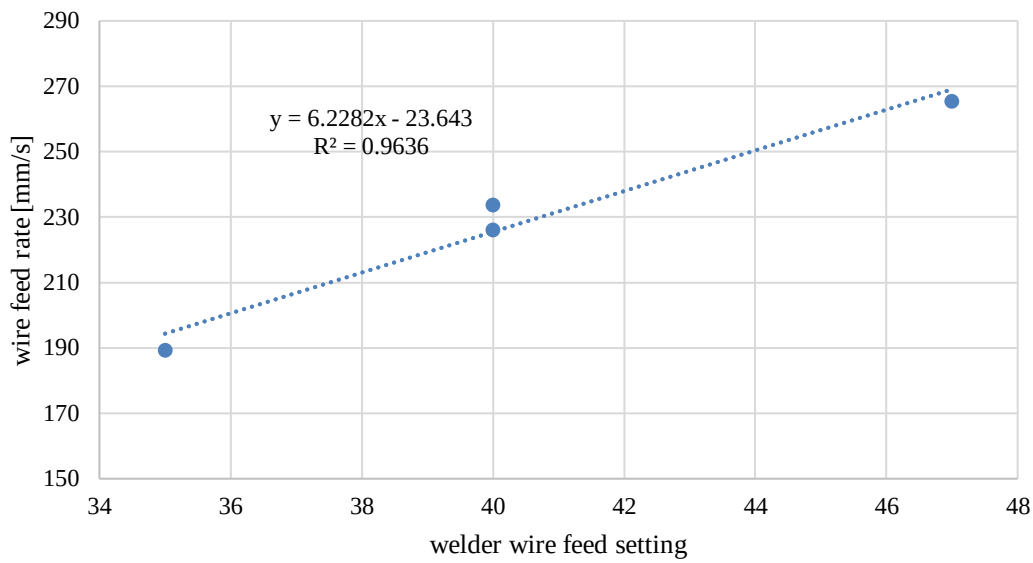

Figure 11. Welder wire feed speed tests with linear fit for approximating wire speed.

When welding aluminum, the position of the torch with respect to the plate is important. Usually, a height of 19mm and push angle of 10-15° is used [63]. For the welding printer a similar height was approximated, but no angle was used. To obtain consistent results regardless of print orientation an angle of 0° was used. This could be changed and researched in the future to improve results.

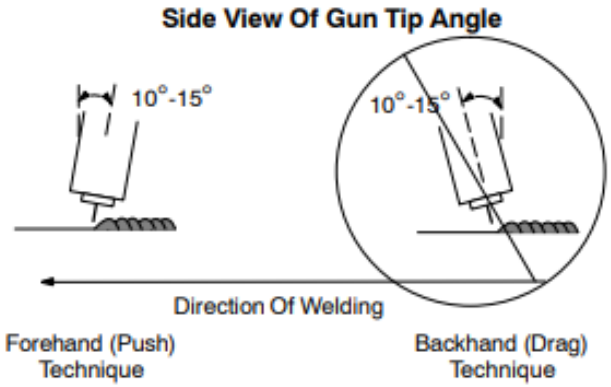

Figure 12. Recommended angle of welding torch [63].

Initially, 1-D welds, or simple lines of weld, were produced for a wide array of settings. The welds that are not desirable based on visual appearance – overpenetration, under penetration, undesirable transfer of feedstock to base metal, slow travel speed – were dismissed from further testing. Further examination of samples with a North Star Imagining (NSI) X View CT M5000 x-ray system revealed some samples having high levels of porosity. Porosity is expected to cause issues in welded parts and reduce mechanical properties, so these welding parameters were not included in further testing. 1D weld test samples dismissed from further testing are shown in figure 13.

Figure 13. North Star Imagining (NSI) X View CT M5000 [64].

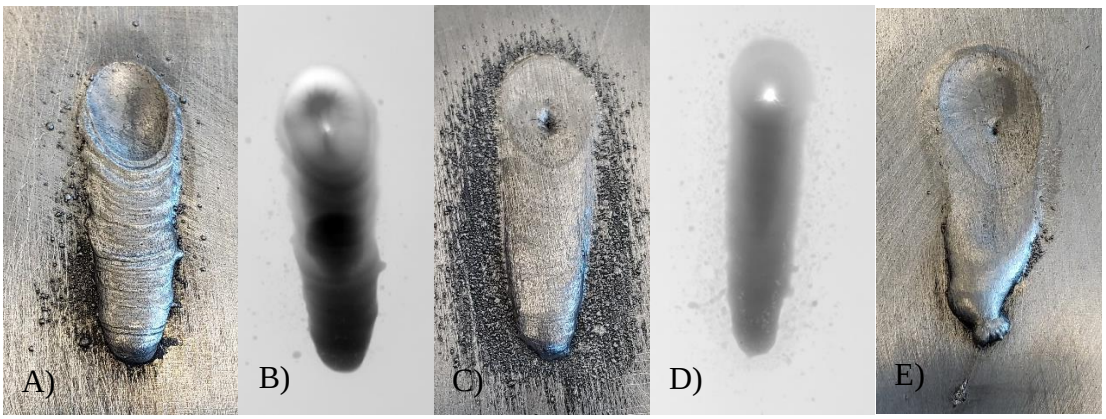

Figure 14. A) & B) Weld eliminated because of inconsistencies, poor penetration, and slow speed. C) & D) Weld eliminated due to high porosity observed along edges of weld shown in image D). E) Weld eliminated based on extreme over penetration.

1D weld settings that performed better were used to create a 2D welds, or lines of weld laid next to one another. Samples were examined both visually and through x-ray to determine the quality. Common problems with 2D welds were over penetration due to increased weld length and concentrated heating, incorrect weld spacing, and welds that did not have enough material due to not enough feed stock and/or welder speed being too fast. Images from 2-D weld testing are shown in figure 15. Settings that performed well in 1D test did not always perform well in 2-D tests.

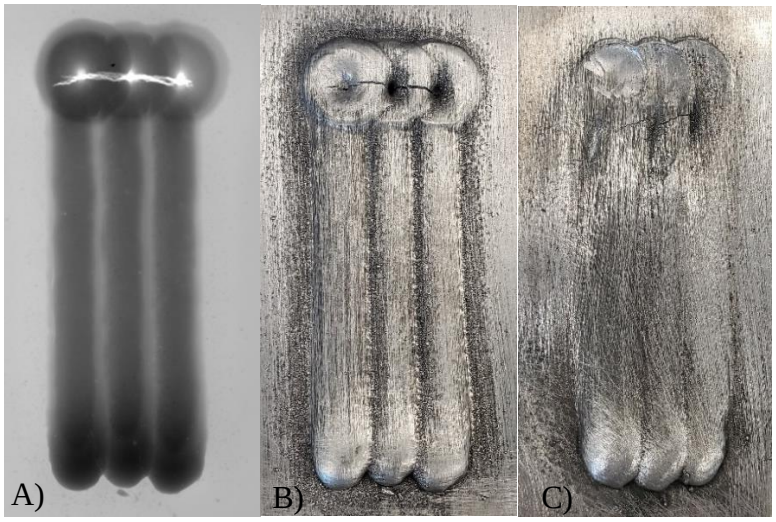

Figure 15. A) & B) Welds eliminated because of large spaces between welds and porosity. C) Weld eliminated due to severe over penetration.

After determining the best 2-D weld settings 3D samples are welded. 3D welds are created by using 2-D layers that are added to the previous layer. Porosity is expected to differentiate the better welder settings from other undesirable welds. To observe porosity along a plane within the samples, they must be cross sectioned along the plane to expose the desired surface. Samples were stabilized in an epoxy resin making the sample easier to polish. Once the sample is stable and solidified the exposed surface is polished using a Pace Technologies Nano 2000T grinder-polisher. Starting with 600 grit sanding pad and working up to a 1200 grit the surface of the sample is wet sanded smooth and to remove any large scratches. After wet sanding, the samples are polished with a diamond suspension starting at a size of 6μm and ending at 0.25 μm. At this point, the surface has little to no scratches, but it is then polished using a silicate suspension to bring the surface to a true mirror finish. Once the sample has been polished, it can be observed under a microscope. The Keyence VHX-600 digital microscope was used to observe porosity. Determining if there is a difference in porosity at the beginning or end of the weld was the first concern. To determine if porosity varies throughout a weld, samples are taken from the beginning, middle, and end of a welded part and then examined. Ten images per sample at random locations over the surfaces were taken. These images were processed with ImageJ to determine porosity.

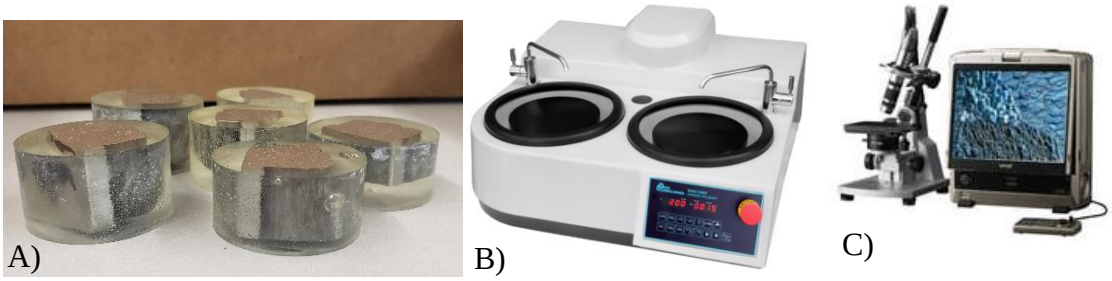

Figure 16. A) Samples for polishing. B) Pace Technologies Nano 2000T grinder-polisher [65]. C) Keyence VHX-600 digital microscope [66].

ImageJ adjusts the microscope images to differentiate pores from aluminum and outputs information about all the pores. To obtain information about pores in the image, the scale was set using the scale on the image. This known distance converts pixels of the image to a linear dimension (μm). The image is converted to 32 bit and a histogram/threshold is adjusted to highlight the darker regions of the image. For this case, the dark regions are pores. Settings are adjusted to include any size pore and all pore shaped imperfections. The summary of the results gives a percentage of the image that is pores as opposed to aluminum. This percentage of pores over the area is an indication of porosity. This method is an approximation because it only examines a small area of a plane of a weld. An example of ImageJ process and results are shown in figure 17.

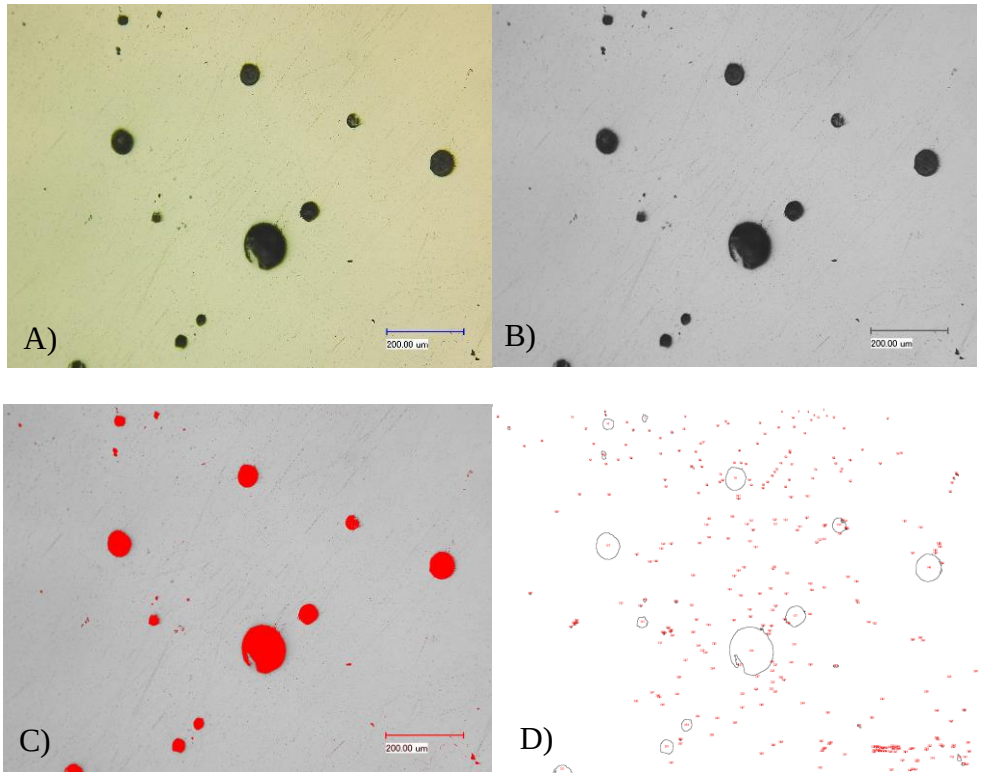

Figure 17. A) Original microscope image. B) Image is converted to 32bit. C) Threshold is used to differentiate pores. D) After determining the size and shape of pores to be observed information is output as a table of values.

Further porosity tests were completed at different welder settings to determine the best welder setting. Statistical analysis was performed to objectively determine if the results were significantly different. Upon initial examination of these samples, trends in porosity seemed to occur throughout the 3D welded aluminum.

To better understand weld porosity in a 3D printed part microscope images were taken in a series of vertical and horizontal regular patterns. Samples were oriented in the microscope so that motion was in line with the layers of weld. Vertical images were taken from the root up and where the edges (toes) of the welds meet and are referred to as the trough and seam, respectively. The horizontal images are taken across the three lines of weld. Images were carefully taken so that if laid out together they could make one continuous image. Figure 18 shows how these images were collected.

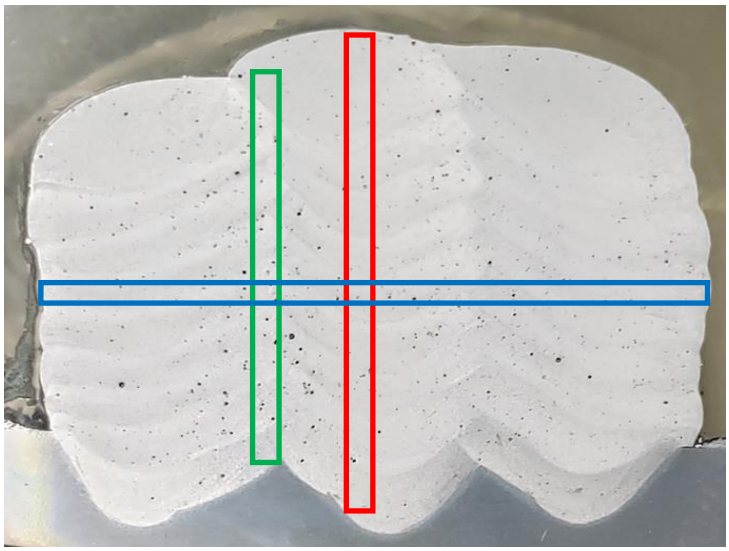

Figure 18. Green represents approximate location of seam images, red trough images, and blue horizontal images.

Settings found to work well for metal 3D printing coincided closely with the recommended settings for the welder and those recommended in MTU and a WAAM printer from China [52][62]. Tables 3 & 4 shows the recommended welder settings along

with settings used during welding the samples for the remaining tests. 3D welding amperage settings were slightly lower as to reduce the change of overpenetration in higher layers.

Table 3. Recommended welder settings [67].

		shielding gas		0.075"/2mm		1/8"/3.2mm		3/16"/4.8mm		1/4"/6.3mm	
wire type	polarity setting	20-30 cfh	diameter of wire	voltage setting	wire feed setting	voltage setting	wire feed setting	voltage setting	wire feed setting	voltage setting	wire feed setting
5356	DC Electrode Positive	100% argon	0.035"/ 0.9mm	4	36	7	44	8	46	9	54

Table 4. Welder settings as tested.

argon [cfh]	welder current setting	wire feed rate	travel speed [mm/s]	distance between welds [mm]	layer height	Torch Height [mm]	Torch Angle [°]	Base Material Thickness [mm]
25	8	40	15	6	1.7	15	0	6.35

In addition to porosity, grain structure can help understand the behavior of a material. To help reveal the grain structure, an etching process is used. Referring to an etchant database by Pace Technologies, the ASTM No. 2 etchant was selected for the samples. The etchant consists of 1g NaOH and 100mL deionized water. The prescribed etching process is to swab the surface for 10 seconds to reveal general structure or to submerse the sample for 15 minutes for hatching based on orientation [68][69]. Neither of these etching methods yielded meaningful results when using an optical microscope. The 10 second swab did not appear to have any impact on the surface and 15 minutes of immersion left nothing recognizable. Etching the sample by immersing it for 2-3 minutes

gave better results. For evaluating grain structure, a Keyence VK-9710 laser microscope was used.

Figure 19. Keyence VK-9710 laser microscope [70].

A good indicator as to whether this method of manufacturing is valid for prototyping and production parts is to perform a tensile test on the material. To prepare, samples for material testing samples are printed in 3 orientations. Welds will be tested by applying load along the path of the weld, perpendicular to the path of the weld and vertical through the welds. Figure 20 illustrates how the samples are to be tested based on these three principal directions.

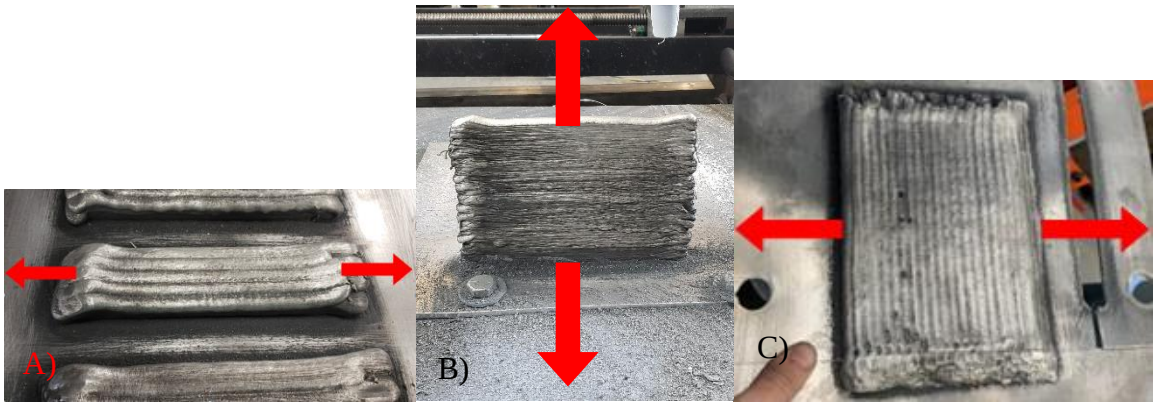

Figure 20. A), B), & C) Sample set A, B, & C respectively after 3D welding. Red arrows show direction that tensile force will be applied.

Samples of 3D welded aluminum are roughly milled to the proper dimensions then CNC milled to the tensile sample geometry. To remove the sample from the plate, the sample is held in a vice and the plate is machined away. The vertical tensile tests were made by removing the welded part from the build plate then securing it in the mill. After the mill produced the necked down region of each sample, the plate was machined on either side. Samples were then cut apart for testing. The process of how tensile tests were made is shown in figure 21. All tensile samples and tests were performed in accordance with ASTM E8/E8M & B557M standards [71][72].

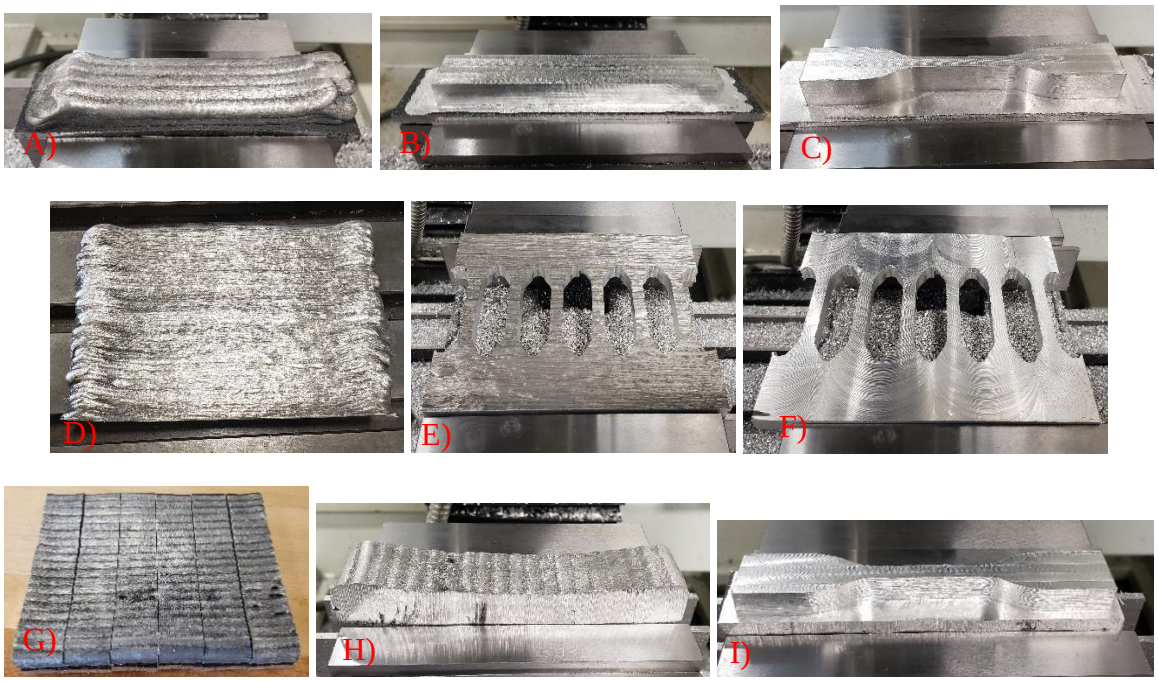

Figure 21. A), B), & C) Set A sample being made. D), E), & F) Set B samples being made. G), H), & I) Set C sample being made.

Figure 22. Samples A, B, & C ready for tensile tests.

Tensile tests were performed using an MTS Landmark to determine the material characteristics of the 3D welded material. Samples are secured in the wedges and an extensometer is attached to the test region of the sample to measure elongation. The test is then run by increasing the distance between the wedge grips at a constant speed of 1.3 mm/min. Time, force, total elongation, and extensometer readings are recorded through the test at 25 Hz. Figure 23 shows the MTS machine and a sample being tested.

Figure 23. Sample in wedges of MTS Landmark Servohydraulic Test System.

The data recoded from the machine is then analyzed using a Matlab script to interpret the results. The Matlab script uses the raw data to calculate ultimate tensile strength, yield strength, maximum elongation, and modulus of elasticity.

The equations used for calculating stress, strain, modulus of elasticity, and elongation are shown below. Where σ is stress, F is force, A is area, ε is strain, δ is change in length, L is the starting length, and E is modulus of elasticity. The ultimate stress occurs at the max force during the tensile test. Yield stress is the force when the sample is no longer in the elastic region, in this case, 0.2% yield stress is calculated. The fracture surface will be examined with a microscope to determine the mechanism of failure.

$$\sigma = \frac{F}{A} \tag{1}$$

$$\varepsilon = \frac{\delta}{L} \tag{2}$$

$$E = \frac{\sigma}{\varepsilon} \tag{3}$$

RESULTS

Results from the initial porosity test to determine whether location in the weld would affect the porosity are shown in table 5. There is not enough significant evidence to suggest that the porosity varies greatly throughout the weld. This means that regardless of where the welded sample is taken the results should yield similar results elsewhere in the same sample.

Table 5. Statistical analysis of porosity throughout a 3D welded aluminum part.

Sample Location	Average Porosity (% area)	Sample Standard Deviation	P-value, compared to start 1	P-value, compared to start 2	P-value, compared to middle	P-value, compared to end 1	P-value, compared to end 2
start 1	1.71	1.11		0.280	0.221	0.495	0.905
start 2	1.28	0.50	0.280		0.789	0.074	0.134
middle	1.22	0.49	0.221	0.789		0.057	0.085
end 1	2.07	1.18	0.495	0.074	0.057		0.349
end 2	1.67	0.59	0.905	0.134	0.085	0.349	

The tests performed to determine porosity vs welder settings are shown in table 6. Upon initial inspection samples 9, 3, and 4 seem to have an advantage over the other samples' weld settings. Statistically, the samples 9, 3, and 4 are not significantly different from one another and samples 4 and 3 are not significantly different from other welder settings. So, there is no discernible advantage to using one of the welder settings over another. For some perspective GE states its AM metal parts have 0.5% porosity if the process is precisely controlled [73], while other research suggests other metal AM methods are in the range of 1-2% [74].

Table 6. Analysis of welder settings vs porosity.

sample	welder current setting	approximate wire speed (mm/s)	travel speed (mm/s)	distance between welds (mm)	layer height (mm)	mean porosity (% area)	std dev	t-test: p-value vs initial	t-test: p-value vs s1	t-test: p-value vs s3	t-test: p-value vs s4	t-test: p-value vs s6	t-test: p-value vs s7	t-test: p-value vs s8	t-test: p-value vs s9
initial	7	225	15	6.2	2.2	1.41	1.08		0.514	0.171	0.431	0.058	0.392	0.662	0.047
s1	9	250	20	6.6	2.32	1.58	1.17	0.514		0.037	0.155	0.199	0.881	0.777	0.007
s3	8	250	25	6	1.7	1.16	0.74	0.171	0.037		0.655	0.001	0.013	0.038	0.451
s4	8	225	15	7	1.7	1.26	1.12	0.431	0.155	0.655		0.010	0.093	0.196	0.297
s6	8	250	20	7	1.7	1.88	1.33	0.058	0.199	0.001	0.010		0.219	0.099	0.000
s7	8	225	20	6	1.8	1.57	0.98	0.392	0.881	0.013	0.093	0.219		0.631	0.001
s8	8	250	20	6	1.8	1.47	0.92	0.662	0.777	0.038	0.196	0.099	0.631		0.005
s9	8	225	15	6	1.8	1.05	0.68	0.047	0.007	0.451	0.297	0.000	0.001	0.005	

The porosity at different features in the welded parts are observed to gain a better understanding of tendencies for porosity in 3D welded parts. An analysis of the porosity in the seam and trough are shown in figure 24 and table 7. There is significant evidence to suggest that the porosity in the trough is not only different, but lower than that of the seam.

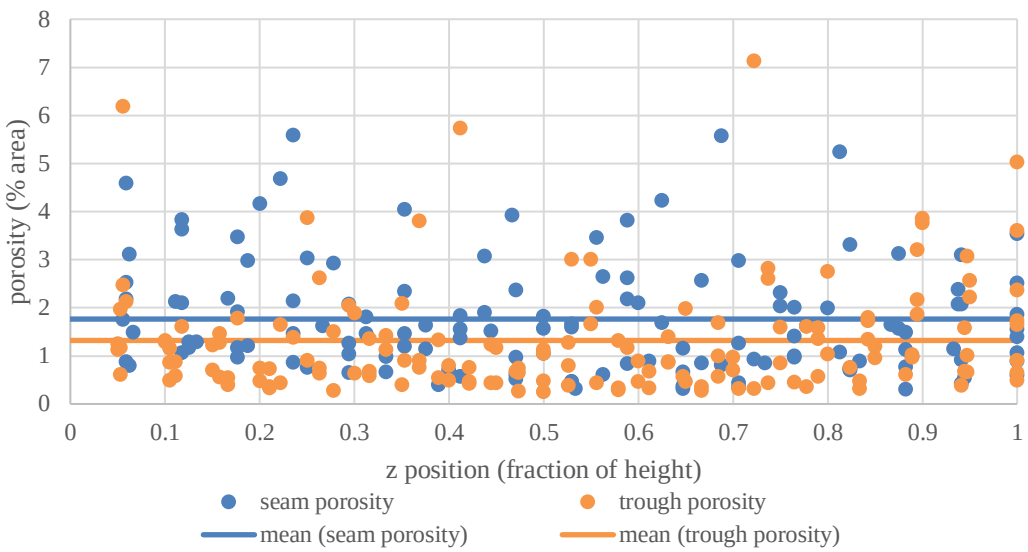

Figure 24. Seam vs trough porosity data.

Table 7. Seam vs trough porosity analysis.

seam porosity		trough porosity	
mean (% area)	1.77	mean (% area)	1.32
std dev	1.17	std dev	1.15
t-test: p-value		0.0007	

To better illustrate this phenomenon of the welds' edges containing more porosity than the roots, the welds are examined horizontally in figures 25 - 28. The variability, or residual, of porosity in the seams of the welds is much higher than that of the roots. It can be said that there is variability across the entire sample, however, it is much more apparent and prominent in the seams. When a polynomial fit is given to each weld, it

closely matches the corresponding seam and trough mean values. Porosity follows the polynomial trend in each weld and shows evidence of higher porosity along the seam than in the root of the weld.

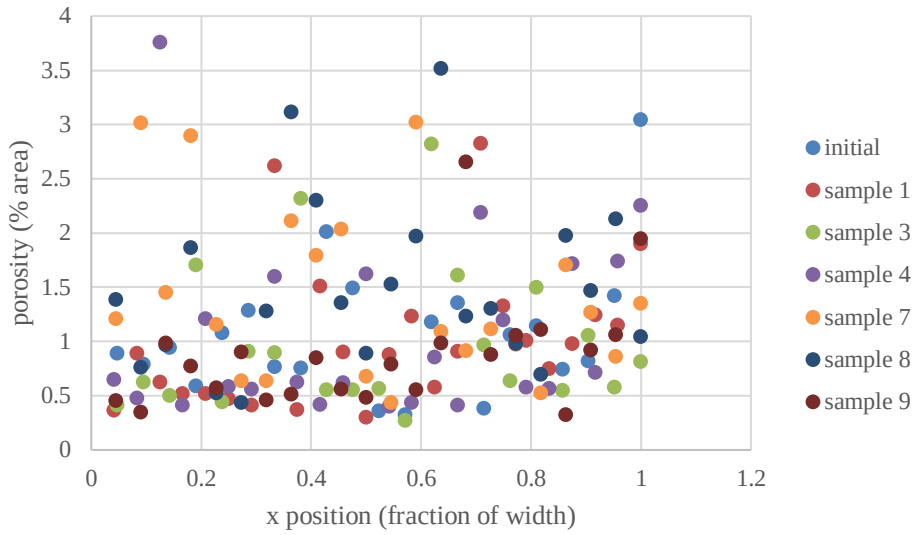

Figure 25. A scatterplot of all porosity measurements for all samples across the sample horizontally.

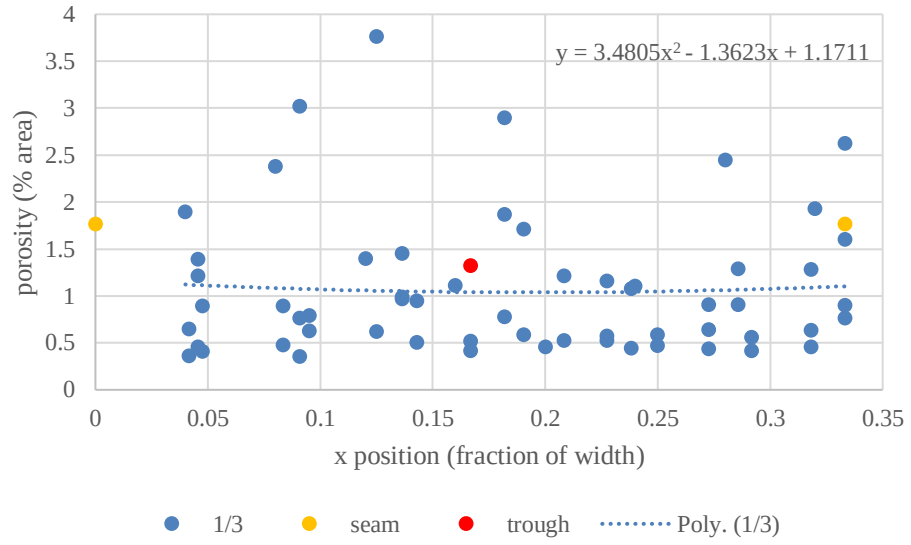

Figure 26. First weld in all samples with a polynomial fit and mean seam and trough porosity values.

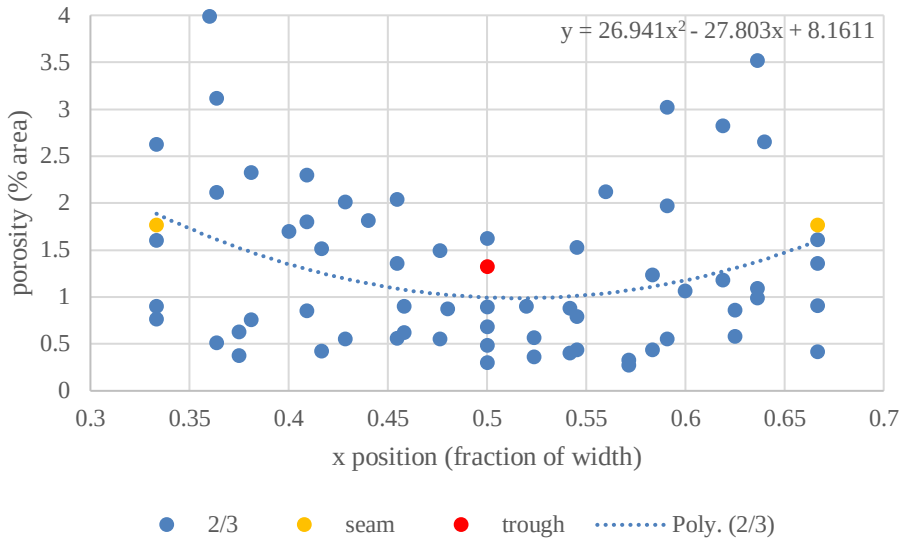

Figure 27. Second weld in all samples with a polynomial fit and mean seam and trough porosity values.

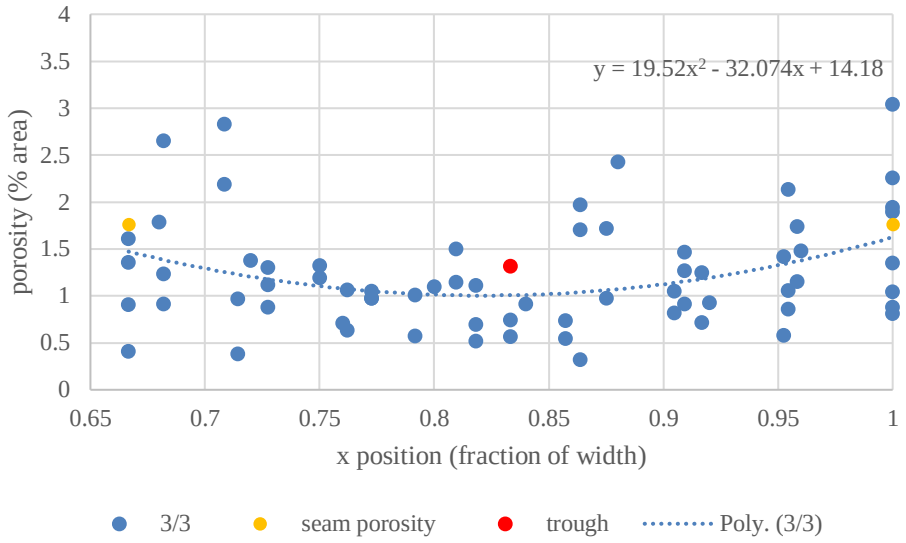

Figure 28. Third weld in all samples with a polynomial fit and mean seam and trough porosity values.

Grain structure can roughly be seen in figure 29. The general regions match those of other researchers that studied the heat affected zone (HAZ), arc zones (AZ), and light strip (LS) [62]. The AZ directly below the HAZ has much smaller grains compared to that above the HAZ.

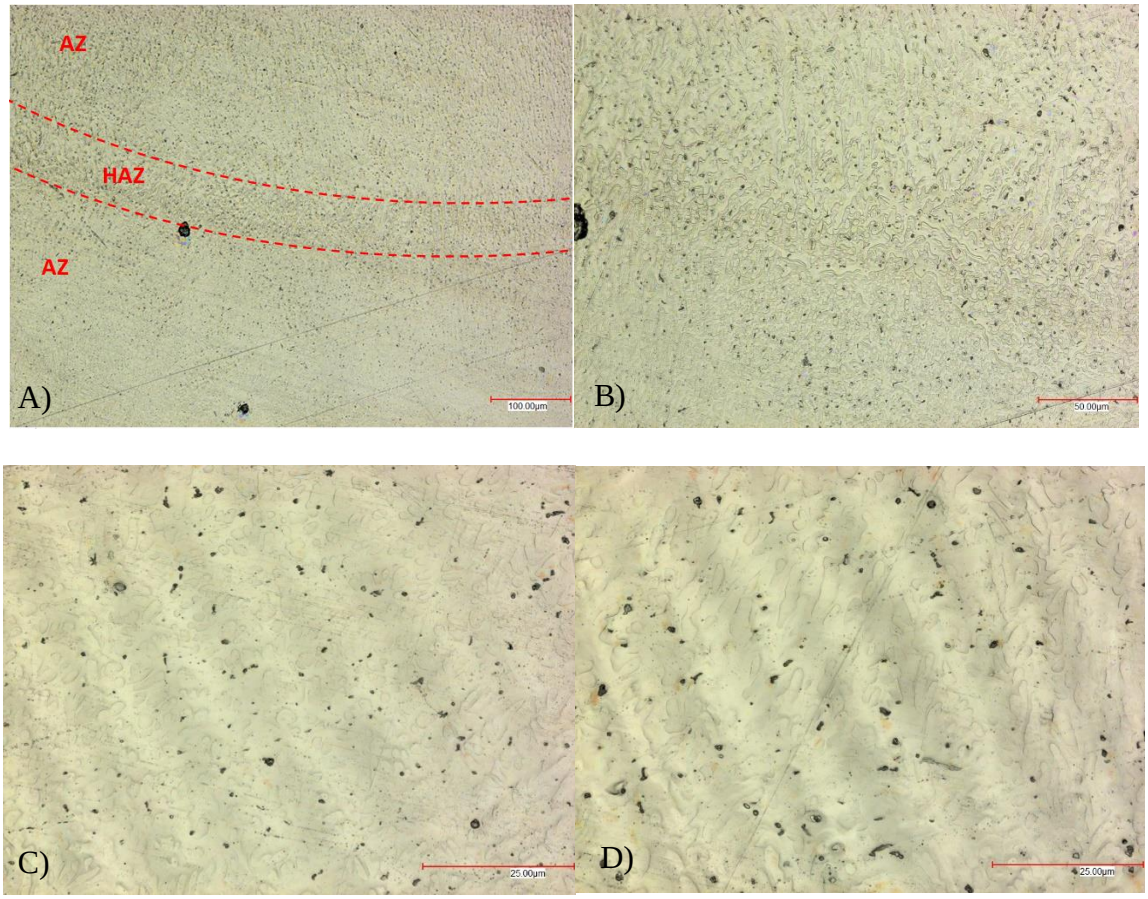

Figure 29. A) Regions within the welded part. B) Transition from AZ to LS to HAZ. C) grain below HAZ. D) Grain above HAZ.

Liquidation cracks can be observed in the HAZ. This is consistent with those in a study of 5356 welding filler [75]. Based on this study, the grain boundaries and small black points in the grains are Al3Mg2. The points within the grain are precipitates which help to harden the material [75].

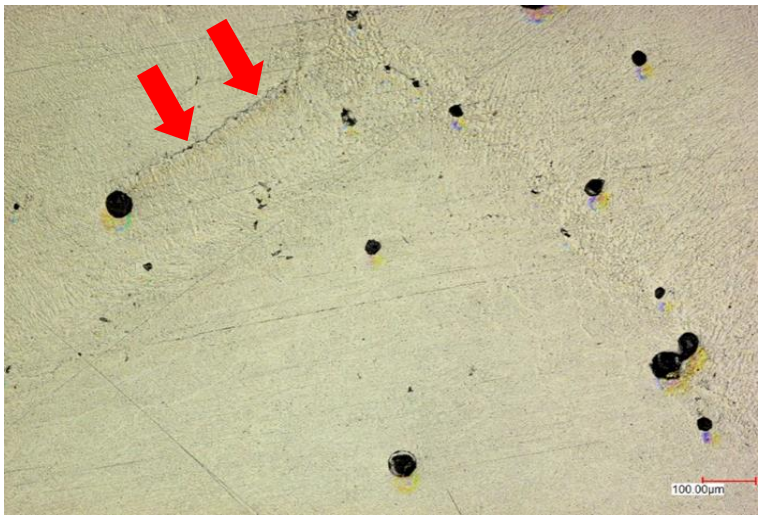

Figure 30. Liquidation cracks where HAZ meets.

Destructive testing in the form of tensile tests were used to determine mechanical properties of the welded aluminum. After analyzing the raw data, the results are shown in the tables and figures below. The tables show ultimate stress, modulus of elasticity, yield stress, and max elongation. Samples A2-A5 exceeded the extensometers max limit. The figures show the stress strain curves of each group of samples.

Table 8. Tensile results for specimens from group A.

Sample Name	Tensile Orientation	Width	Thickness	Ultimate Stress [MPa]	Modulus of Elasticity [GPa]	Yield Stress [MPa]	Max Elongation [%]
A1	along	0.232	0.292	283.68	68.45	131.11	21.19
A2	along	0.234	0.298	289.95	69.94	127.75	21.20
A3	along	0.234	0.301	281.18	66.40	127.03	21.26
A4	along	0.233	0.3	280.96	70.17	133.85	21.28
A5	along	0.235	0.275	280.76	69.02	129.92	21.22
A6.5	along	0.235	0.305	269.28	68.21	126.41	18.12
A7	along	0.239	0.26	261.44	68.23	124.71	12.60
mean		0.235	0.290	278.18	68.63	128.68	19.55

Table 9. Tensile results for specimens from group B.

Sample Name	Tensile Orientation	Width	Thickness	Ultimate Stress [MPa]	Modulus of Elasticity [Gpa]	Yield Stress [MPa]	Max Elongation [%]
B1	vertical	0.229	0.235	248.65	59.98	113.13	19.19
B2	vertical	0.229	0.231	236.16	62.56	114.10	15.44
B3	vertical	0.228	0.235	241.68	59.91	111.52	17.04
B4	vertical	0.229	0.233	209.03	61.92	116.16	10.95
B5	vertical	0.229	0.236	227.14	57.63	112.29	10.29
mean		0.229	0.234	232.53	60.40	113.44	14.58

Table 10. Tensile results for specimens from group C.

Sample Name	Tensile Orientation	Width	Thickness	Ultimate Stress [MPa]	Modulus of Elasticity [GPa]	Yield Stress [MPa]	Max Elongation [%]
C1	across	0.233	0.301	229.54	66.03	135.28	6.50
C2	across	0.244	0.303	203.02	63.73	126.34	9.96
C3	across	0.23	0.295	234.30	71.29	142.65	4.96
C4	across	0.233	0.305	206.28	67.74	138.58	3.55
C5	across	0.231	0.3	264.48	68.87	139.49	15.55
C6	across	0.231	0.292	263.30	72.01	142.17	9.23
mean		0.234	0.299	233.49	68.28	137.42	8.29

Table 11. Comparison of 3D welded 5356 aluminum to same welded, wrought, and cast alloy and one DMLS printed AlSi10Mg alloy.

Sample Name	Tensile Orientation	Ultimate Stress [MPa]	Modulus of Elasticity [GPa]	Yield Stress [MPa]	Max Elongation [%]
mean sample A	along	278.18	68.63	128.68	19.55
mean sample B	vertical	232.53	60.40	113.44	14.58
mean sample C	across	233.49	68.28	137.42	8.29
Blue Demon Welding [58]		262			
AZO [59]			70-80		
Harris Welding [60]		269		131	17
5356-O wrought [76]		285		130	
535.0 (AL-6.9Mg) cast [76]		250		124	9
AlSi10Mg DMLS [77]		379	68.3	232	6.9

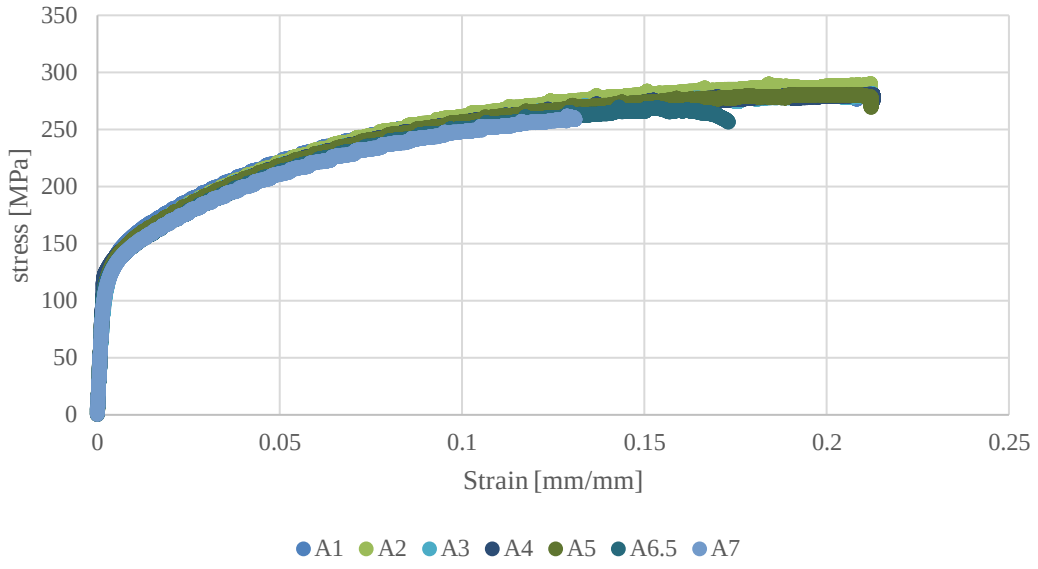

Figure 31. Stress strain curve for A samples.

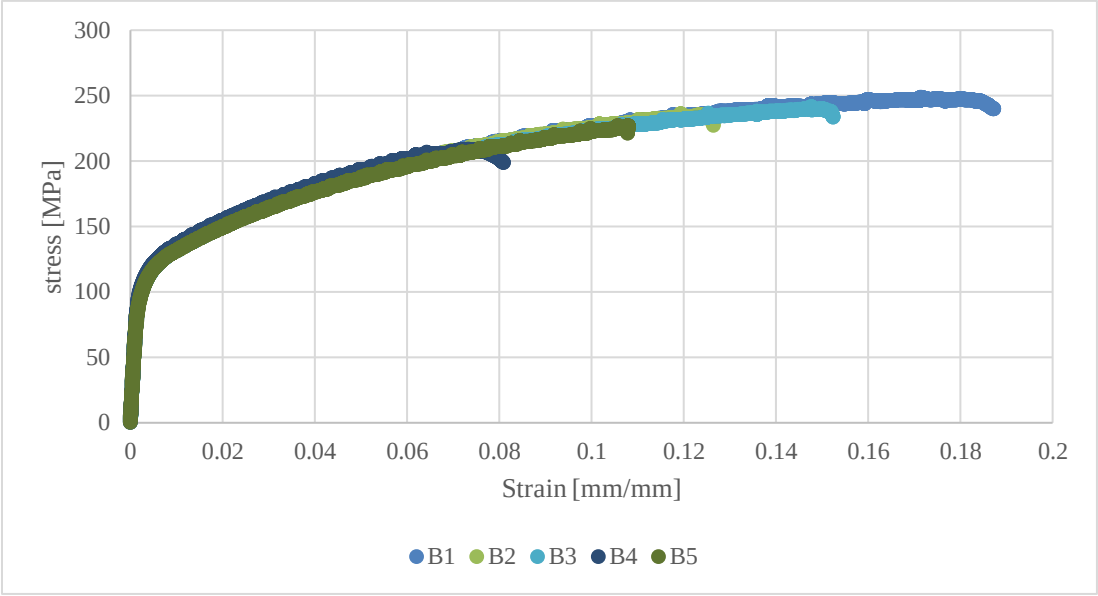

Figure 32. Stress strain curve for B samples.

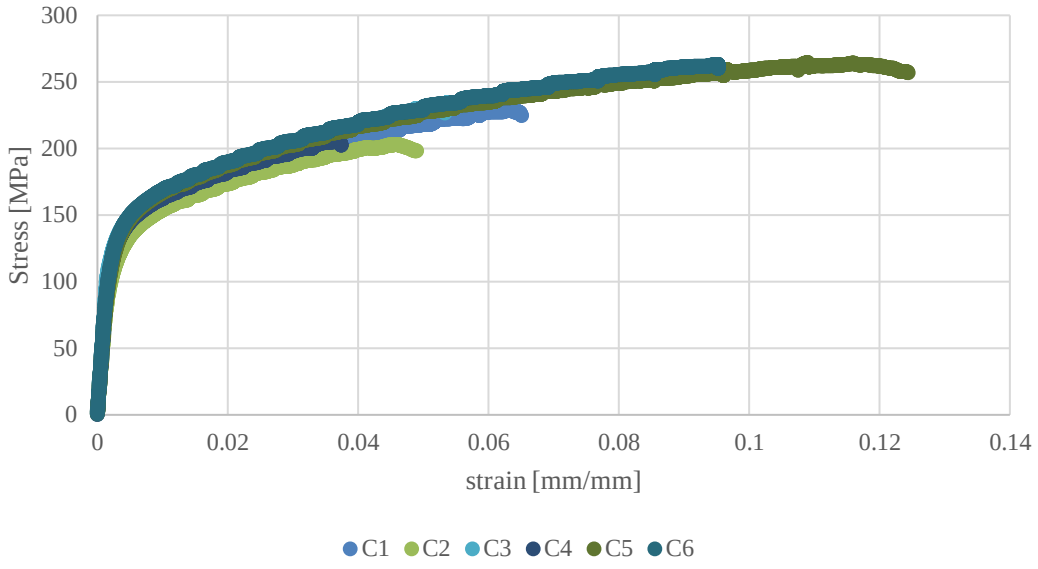

Figure 33. Stress strain curve for C samples.

After tensile tests were complete, the samples' fracture surfaces are examined under a microscope. When taking images of the rough surfaces, some areas are out of focus due to the height difference. The rough surface is an indication of ductile failure which is expected due to the plastic region of the stress strain curves. Images of fracture surfaces are shown in figures below.

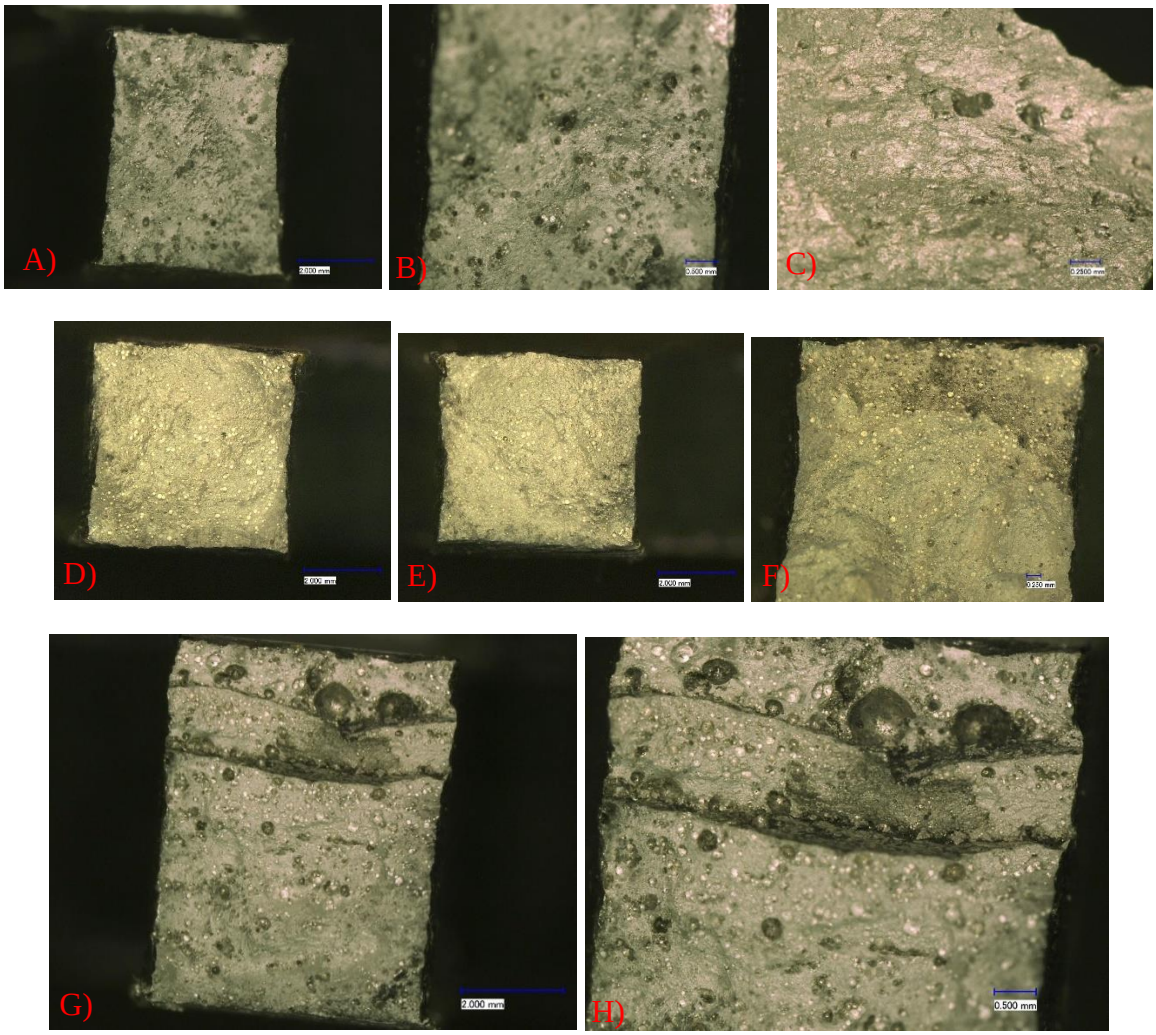

Figure 34. A), B), &C) Fracture surfaces of sample A. D), E), & F) Fracture surfaces of sample B (D and E being either side of the same sample). G) & H) Fracture surfaces for sample C.

DISCUSSION

Porosity in a material is typically thought of as a property of the bulk material. Welding causes properties and characteristics to be highly localized within the material so using an average porosity value is not a good representation of the overall part. Using methods that find total or average porosity is a poor indicator of the materials characteristics. While there was not statistical evidence to show that porosity throughout at welded AM part changes in the different regions, it is still likely that there are differences throughout the part and further study is needed to show that phenomenon. In the testing shown in this paper, the porosity for all welder settings were between 1-2% with welder settings having no meaningful effect on porosity. Significant evidence shows a significant difference for porosity of 3D GMAW parts depending on the location within the weld. It can be said that the porosity in such parts is random, but follows the general trend that porosity tends to be higher towards the edges of a weld.

When determining the porosity of a sample at welder settings, the original method of using ten random images was determined to be inaccurate or insufficient at telling the full details of porosity. While studying this data, it was determined that porosity is local within the welds. When a more regular observation was used, results became more consistent and standard deviation was reduced. The comparison of the mean porosity values and sample standard deviations are shown in table 12. With 90% confidence, the vertical and horizontal method of obtaining porosity values is more consistent and accurate than the ten random sample method.

Table 12. Comparison of two methods of obtaining average porosity values in a sample.

						local (vertical/horizontal)		average (10 random)	
sample	welder current/ voltage	approximate wire speed (mm/s)	travel speed (mm/s)	distance between welds (mm)	layer height (mm)	mean porosity (% area)	std dev	mean porosity (% area)	std dev
initial	7	225	15	6.2	2.2	1.41	1.08	1.59	0.86
s1	9	250	20	6.6	2.32	1.58	1.17	2.60	1.55
s3	8	250	25	6	1.7	1.16	0.74	1.95	1.28
s4	8	225	15	7	1.7	1.26	1.12	1.15	0.52
s6	8	250	20	7	1.7	1.88	1.33	2.58	2.49
s7	8	225	20	6	1.8	1.57	0.98	2.07	1.53
s8	8	250	20	6	1.8	1.47	0.92	1.79	0.94
s9	8	225	15	6	1.8	1.05	0.68	1.69	1.12
mean						1.42	1.00	1.93	1.29
std dev						0.26	0.22	0.49	0.60
1 tail t-test: P-value of local vs average mean						0.003			
1 tail t-test: P-value of local vs average std dev						0.091			

Porosity in welding is difficult to understand and hard to predict. As mentioned above, patterns can be predicted but porosity is random. To further illustrate this concept, studies by Lincoln Welding and MTU have contrasting conclusions based on porosity. Lincoln states that 4043 aluminum is more prone to porosity while MTU studies show the 4000 series aluminum is less porous than the 5356 [78][79]. Both studies provide limited information about how these results were obtained so it is difficult to draw too many conclusions. However, the differences in conclusions of these two studies show that porosity is difficult to study and unpredictable. Adding to this, the porosity in these tests is between 1-2% with a mean of 1.67% and appears slightly lower than the value of 1.85% given by the MTU paper.

Table 13. Lincoln Welding information on ER4043 and ER5356 aluminum alloys [78].

ER4043	ER5356
Higher Penetration	Lower Penetration
Lower Ductility	Higher Ductility
Lower Tensile	Higher Tensile
More Prone to Porosity	Less Prone to Porosity
Much Lower Shear Strength	Higher Shear Strength
Lower Cracking Sensitivity	Higher Cracking Sensitivity
Narrower Melting Range	Wider Melting Range

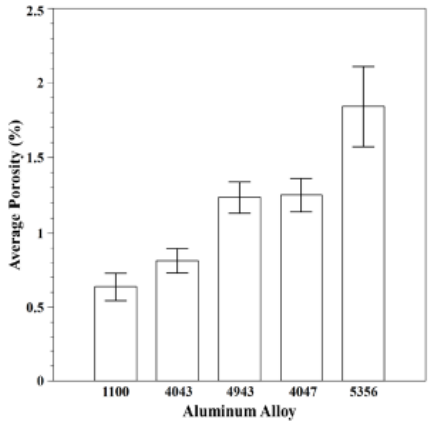

Figure 35. MTU's contrasting results for porosity between 5000 and 4000 series aluminum welding filler wire [79].

Based on the data obtained through tensile tests ultimate strengths, modulus of elasticity, and yield strengths are similar regardless of test orientation. Slight variations could be because of porosity, welding process, or the print pattern. C samples show a lower elongation, and this could be because of the layering mentioned above. The mechanical properties of samples A, B, and C are very consistent based on the stress strain curves. These material behaviors are in line with those of materials provided by welding wire suppliers of welded product [58][60], research done on similar wrought and cast alloy [76], and DMLS of a similar alloy [77]. The welded material meets or exceeds the welded, wrought, and cast alloys in two of the test directions (along the weld and across the weld). The main take away is that using this method, settings, and alloy, 3D welding aluminum is a valid source of additive manufacturing.

The failure mechanism for most samples was simple ductile failure of the material. Few samples displayed failure due to large size pores like the one in figure 36. Samples of the A type (tension along the weld) exhibited a fracture surface at an angle to the direction of applied force. This is expected because metals fail due to shear and the resolved shear occurs at an angle to the applied load. The angle the part failed is likely the orientation of the crystal structure within the part. However, the fracture surface was not always consistent and sometimes the edge had a fracture oriented differently. This could be because of necking, but was localized to a small location and not the entire edge. Additionally, A samples also have a rough looking fracture surface which indicates ductility in the part.

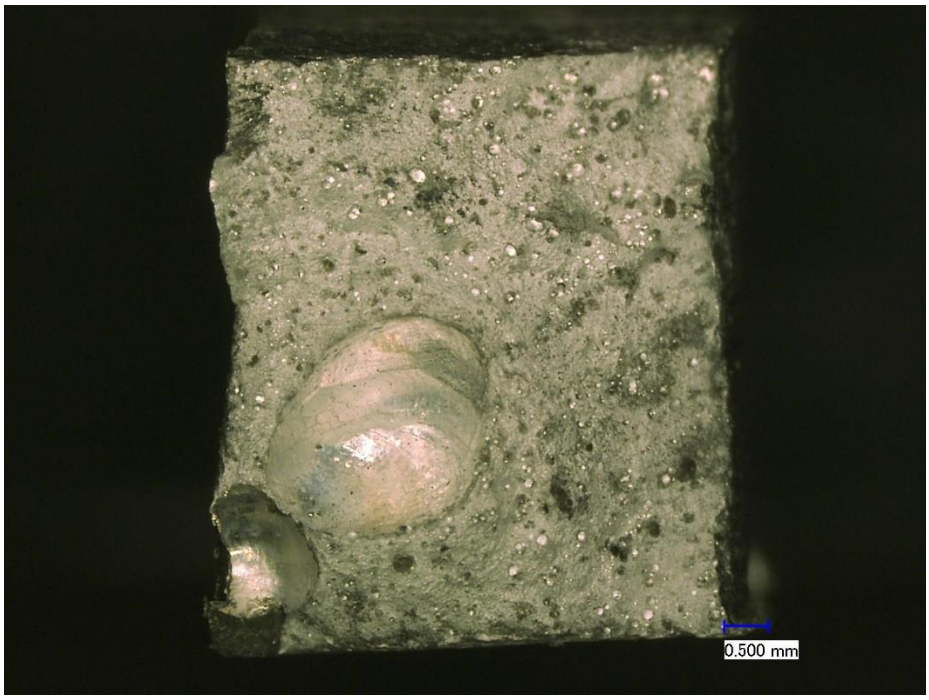

Figure 36. Failure likely due to large pores.

B samples (tension vertical of the weld) showed the same rough fracture surface and necking, both signs of ductile failure. The B samples tended to break orthogonally to the applied load with a rough surface. Overall, these samples displayed ductile fracture characteristics.

C samples (tension across welds) also displayed the same ductile rough fracture surface, but something to note is the regular ridge patterns on the fracture surface. These ridges occurred at intervals that coincide with the layer height and are unique to the C samples. With the fracture surface being generally orthogonal to the direction of the applied load and the ridges suggest that the failure is occurring at the seam where the welds meet. This could be caused by the potential concentration of porosity at this region and/or liquidation cracks. The microscope images do show large pores at these regions, so the potential increased porosity likely lead to failure.

ADDITIONAL WORK

A scanning electron microscope (SEM) analysis could help determine grain structure and composition within the different welded areas. Additional nondestructive testing on parts like x-ray diffraction (XRD), X-ray/CT (according to ASTM E1814), hardness and microhardness, ultrasonic, and electromagnetic testing could also lead to a better understanding of the material. The XRD and other residual stress tests can determine how much internal stress is in the part as it cools and begins to shrink and warp. Destructive tests like bending (ASTM E290), impact (ASTM E23 and E2298), and fatigue (ASTM E606 and E466) could be performed to understand how a 3D welded part may fail.

Making tensile samples with the rough welded surface exposed and prepared so no internal stresses are relieved could lead to advancements in how the part is made. For example, if a part needs to be strong and milling the rough surface away decreases part strength, then leaving extra material is a positive effect. Experimenting with how print orientation and patterns affect the strength or residual and internal stresses could result in better print methods and stronger bulk material. Tests on slicing techniques that control the weld patterns and alternate weld start locations could influence warping of the base material and reduce weak or high porosity areas. The addition of a water-cooled bed may also help reduce warping.

Some 3D printed metals are heat treatable so more layers can produce different material characteristics as the layers increase. ER 5356 is not a heat treatable alloy of aluminum, but trying tests at different layers may reveal other valuable information about the printed aluminum's characteristics [80]. Large scale prints need to be tested to see if

the characteristics change on a larger scale. Researching porosity's effects on strength could determine if porosity is a driving factor in optimizing welder settings. Additional tests could be run at other travel speeds to determine if speed affects strength again aiding in welding optimization. If the part does not lose much strength, then faster print speeds are desirable to decrease print times.

Reintegrating the stepper motor wire feed assembly would give the printer the ability to finely control feed rate as the printer accelerates. This would allow for the printer to move using regular kinematics and allow for a more consistent weld geometry throughout a weld and an entire print. After integration, the correct slicer settings need to be established for the welding process to yield sliced parts capable of being printed. MTU's slicer software could prove valuable for faster and easier welding parts of a job. A goal would be to create a slicer that could incorporate the use of the spindle or macro that could combine milling and printing g-codes. Doing so would make the printer easier to use and more functional.

After testing is complete on Blue Demon 5356 aluminum, other manufacturers' 5356 aluminum, other aluminum alloys, or steel could be tested to see how it compares. Advanced research could go in to implementing 4th and 5th axis control or adding weld monitoring with a close loop feedback system for wire feed and travel speed. If a 4th and/or 5th axis of control was added tests could determine the best torch angle and position during a weld. An improvement would be to start the flow of shielding gas before the beginning of a weld or creating a print chamber to control the environment around the weld.

CONCLUSIONS

Existing metal AM methods are costly and have some limitations. An open-source hybrid metal printer would aim to produce large parts quickly and efficiently. 3D welding aluminum could be a cost-effective option for high metal deposition rate while a milling spindle would create dimensional accuracy. ER5356 is a readily available aluminum welding wire chosen for its mechanical and physical properties. Welder settings for 3D welding aluminum are similar to that recommended by the welder's manual. Porosity within a welded part is not statistically different from beginning to end of a weld. However, the porosity is expected to be greater where welds meet and is local within a welded part. Tensile tests on 3D welded 5356 aluminum suggests that the process may be capable of producing prototypes and some production parts. The mechanical properties of 3D welded 5356 is expected to have properties that are local to the welds within the part like that of the porosity. Based on the observations from these tensile samples, it is likely that mechanical properties, like porosity, are local within the welded part. Further testing is needed to confirm the full capabilities and characteristics of 3D welded 5356.

LITERATURE CITED

[1] Ultimaker Cura 4.7 [Computer software]. (2020). Retrieved from https://ultimaker.com/software/ultimaker-cura

[2] Abdulhameed, Osama, Al-Ahmari, Abdulrahman, Ameen, Wadea, & Mian, Syed Hammad. (2019). Additive manufacturing: Challenges, trends, and applications. Advances in Mechanical Engineering, 11(2), 168781401882288. https://doi.org/10.1177/1687814018822880

[3] Goldberg, Dana, et al. "History of 3D Printing: It's Older Than You Think [Updated]." *Redshift EN*, 21 Dec. 2018, redshift.autodesk.com/history-of-3d-printing/.

[4] "The History of 3D Printing: From the 80s to Today." *Sculpteo*, www.sculpteo.com/en/3d-learning-hub/basics-of-3d-printing/the-history-of-3d-printing/.

[5] MANUFACTUR3D. "How Stereolithography (SLA) 3D Printing Works?" *MANUFACTUR3D*, 12 July 2020, manufactur3dmag.com/stereolithography-sla-3d-printing-works/.

[6] Oceanz, Sales. "How to Design Parts for SLS 3D Printing." *3D Hubs*, www.3dhubs.com/knowledge-base/how-design-parts-sls-3d-printing/.

[7] O'Neal, Bridget. "ABS: Researchers Test Temperature & Speed Settings in FDM 3D Printing - 3DPrint.Com: The Voice of 3D Printing / Additive Manufacturing." *3DPrint.Com | The Voice of 3D Printing / Additive Manufacturing*, 20 Feb. 2019,

3dprint.com/236571/abs-researchers-test-temperature-speed-parameters-3d-printing/.

[8] Afzal, Sayeed. (2018). Different types of manufacturing processes | the 'all in one' guide. Linked in. https://www.linkedin.com/pulse/different-types-manufacturing-processes-all-one-guide-sayeed-afzal

[9] "What Are the Advantages of Metal 3D Printing?" *Beamler*, 23 Feb. 2021, www.beamler.com/what-are-the-advantages-of-metal-3d-printing/.

[10] Kreiger, Megan, and Joshua M. Pearce. "Environmental Life Cycle Analysis of Distributed Three-Dimensional Printing and Conventional Manufacturing of Polymer Products." *ACS Sustainable Chemistry & Engineering*, vol. 1, no. 12, 2013, pp. 1511–1519., doi:10.1021/sc400093k.

[11] Hällgren, Sebastian, et al. "Additive Manufacturing and High Speed Machining - Cost Comparison of Short Lead Time Manufacturing Methods." *Procedia CIRP*, vol. 50, 2016, pp. 384–389., doi:10.1016/j.procir.2016.05.049.

[12] Renzenbrink, Tessel. "3D Printing Beats Mass Production In Energy Efficiency." *Elektor*, 25 Mar. 2021, www.elektormagazine.com/articles/3d-printing-beats-mass-production-in-energy-efficiency#:~:text=and%20green...-,A%20study%20from%20Michigan%20Technology%20University%20shows%203D%20printed%20products,than%20large%2Dscale%20manufactured%20goods.&text=Another%20important%20factor%20is%20the%20improved%20material%20efficiency%20of%20additive%20manufacturing.

[13] Liu, Zhaobing, et al. “Mechanical Characteristics of Wood, Ceramic, Metal and Carbon Fiber-Based PLA Composites Fabricated by FDM.” *Journal of Materials Research and Technology*, vol. 8, no. 5, 2019, pp. 3741–3751., doi:10.1016/j.jmrt.2019.06.034.

[14] Jagoda, Jeneé, et al. “The Viability and Simplicity of 3D-Printed Construction: A Military Case Study.” *Infrastructures*, vol. 5, no. 4, 2020, p. 35., doi:10.3390/infrastructures5040035.

[15] Stratton, Scott, Manoukian, Ohan S, Patel, Ravi, Wentworth, Adam, Rudraiah, Swetha, & Kumbar, Sangamesh G. (2018). Polymeric 3D printed structures for soft-tissue engineering. *Journal of Applied Polymer Science*, *135*(24), 45569–n/a. https://doi.org/10.1002/app.45569

[16] Karayel, Elif, and Yahya Bozkurt. “Additive Manufacturing Method and Different Welding Applications.” *Journal of Materials Research and Technology*, vol. 9, no. 5, 2020, pp. 11424–11438., doi:10.1016/j.jmrt.2020.08.039.

[17] *Relativity Space*, www.relativityspace.com/.

[18] Albright, Brian. “Siemens 3D Prints Power Turbine Blades.” *Digital Engineering*, 12 June 2017, www.digitalengineering247.com/article/siemens-3d-prints-power-turbine-blades/.

[19] Caiazzo, Fabrizia, et al. “Laser Powder-Bed Fusion of Inconel 718 to Manufacture Turbine Blades.” *The International Journal of Advanced*

Manufacturing Technology, vol. 93, no. 9-12, 2017, pp. 4023–4031., doi:10.1007/s00170-017-0839-3.

[20] Chen, Wan, Lu, Chihua, & Liu, Zhien. (2020). Optimal Design of a 3D Printed Composite Micro-Perforated Silencer for Engine Intake Noise Control. *IOP Conference Series. Materials Science and Engineering*, *774*(1), 12125. https://doi.org/10.1088/1757-899X/774/1/012125

[21] "Local Motors Unveils Designs for 3D-Printed Car Production Line · Local Motors." *Local Motors*, 14 June 2017, localmotors.com/press-release/local-motors-unveils-designs-for-3d-printed-car-production-line/.

[22] Sames, W. J., et al. "The Metallurgy and Processing Science of Metal Additive Manufacturing." *International Materials Reviews*, vol. 61, no. 5, 2016, pp. 315–360., doi:10.1080/09506608.2015.1116649.

[23] "Powder Bed Fusion." Additive Manufacturing Research Group, Loughborough University, www.lboro.ac.uk/research/amrg/about/the7categoriesofadditivemanufacturing/powderbedfusion/.

[24] Sing, S. L., Tey, C. F., Tan, J. H. K., Huang, S., & Yeong, W. Y. (2020). 3D printing of metals in rapid prototyping of biomaterials: Techniques in additive manufacturing. Rapid Prototyping of Biomaterials, 17–40. doi:10.1016/b978-0-08-102663-2.00002-2

[25] "Metal 3D Printing: An Overview of the Most Common Types." *3D Printing*, 14 Dec. 2020, 3dprinting.com/metal/types-of-metal-3d-printing/.

[26] "Joule Printing™ – A Radically Simple New Technology for Fast, Low-Cost Metal Additive Manufacturing." *Digital Alloys*, www.digitalalloys.com/technology/.

[27] "Get the Right 3D Printer or 3D Scanner." *Aniwaa*, www.aniwaa.com/.

[28] Simpson, Timothy W. "Why Does My 3D-Printed Part Cost So Much?" *Additive Manufacturing*, Additive Manufacturing, 7 May 2018, www.additivemanufacturing.media/articles/why-does-my-3d-printed-part-cost-so-much.

[29] "MIG Wire - Aluminum." *Airgas*, www.airgas.com/Welding-Products/Filler-Metal/MIG-Wire-(GMAW-&-SAW)/MIG-Wire---Aluminum/category/156?q=%3Aprice-desc.

[30] "Powder Vs. Wire." *Digital Alloys*, 25 Sept. 2019, www.digitalalloys.com/blog/powder-vs-wire/.

[31] "Economics of Metal Additive Manufacturing." *Digital Alloys*, 17 June 2019, www.digitalalloys.com/blog/economics-metal-additive-manufacturing/.

[32] "Powder Bed Fusion (PBF)." *Digital Alloys*, 17 June 2019, www.digitalalloys.com/blog/powder-bed-fusion/.

[33] Andrews, N., Gradl, P. Mireles, O., Manufacturing for Propulsion Systems. AIAA Joint Propulsion Conference. July 9-11, 2018.

[34] "Direct Metal Laser Sintering [DMLS] Parts On Demand." *Stratasys*, www.stratasysdirect.com/technologies/direct-metal-laser-sintering.

[35] "Markforged Metal 3D Printer: The Metal X 3D Printing System." *Markforged*, markforged.com/3d-printers/metal-x.

[36] "Markforged Metal X: Review the Specs & Use Cases." *All3DP Pro*, 15 May 2020, all3dp.com/1/markforged-metal-x-review-3d-printer-specs/#:~:text=The%20Markforged%20Metal%20X%20comes,%2B%20industrial%20DMLS%2FSLM%20machines.

[37] *"Titomic Kinetic Fusion®."* Titomic, 2021, titomic.com/titomic-kinetic-fusion/.

[38] "ADDITIVE MANUFACTURING Machines from DMG MORI." *Machines from DMG MORI*, us.dmgmori.com/products/machines/additive-manufacturing.

[39] "Arc Machines, Manufacturing of Metallic Components, Welding Process." *GEFERTEC*, www.gefertec.de/en/arc-machines/.

[40] "Our 3-D Metal Printing Featured in Additive Manufacturing Magazine." *Wolf Robotics*, www.wolfrobotics.com/3-d-metal-printing-featured/.

[41] DNewsChannel, director. *These Engineers Want to 3D Print an Entire Rocket in 60 Days*. *YouTube*, Seeker, 19 May 2019, www.youtube.com/watch?v=R5mhUm6NzqE.

[42] "Electron Beam Additive Manufacturing (EBAM®)." *Sciaky*, www.sciaky.com/additive-manufacturing/electron-beam-additive-manufacturing-technology.

[43] *MX3D*, mx3d.com/.

[44] Eric Berger - Jan 17, 2019 4:00 pm UTC. “Relativity Space to Launch from Historic Florida Site.” *Ars Technica*, 17 Jan. 2019, arstechnica.com/science/2019/01/relativity-space-to-launch-from-historic-florida-site/.

[45] Ding, Donghong, et al. “Wire-Feed Additive Manufacturing of Metal Components: Technologies, Developments and Future Interests.” *The International Journal of Advanced Manufacturing Technology*, vol. 81, no. 1-4, 9 May 2015, pp. 465–481., doi:10.1007/s00170-015-7077-3.

[46] “First Test - Metal 3D Printer.” *YouTube*, YouTube, 16 Oct. 2014, www.youtube.com/watch?v=HuecoWOo2l4.

[47] Gerlich, Adrian, director. *Metal Maker 3D Printer via Welding*. *YouTube*, YouTube, 21 Dec. 2016, www.youtube.com/watch?app=desktop&v=odGEzRRDfxo.

[48] IvánTabernero, et al. “Study on Arc Welding Processes for High Deposition Rate Additive Manufacturing.” *Procedia CIRP*, vol. 68, 23 Apr. 2018, pp. 358–362., doi:10.1016/j.procir.2017.12.095.

[49] Anzalone, Gerald C., et al. “A Low-Cost Open-Source Metal 3-D Printer.” *IEEE Access*, vol. 1, 9 Dec. 2013, pp. 803–810., doi:10.1109/access.2013.2293018.

[50] Pinar, A., et al. “Low-Cost Open-Source Voltage and Current Monitor for Gas Metal Arc Weld 3D Printing.” *Journal of Sensors*, vol. 2015, 30 Aug. 2015, pp. 1–8., doi:10.1155/2015/876714.

[51] Nilsiam, Yuenyong, et al. “Slicer and Process Improvements for Open-Source GMAW-Based Metal 3-D Printing.” *Additive Manufacturing*, vol. 18, 5 Oct. 2017, pp. 110–120., doi:10.1016/j.addma.2017.10.007.

[52] “CNC Router Parts-Based Metal Printers SOP.” *Appropedia*, www.appropedia.org/CNC_Router_Parts-based_metal_printers_SOP.

[53] “CNC Router Parts Metal 3D Printer.” *Appropedia*, www.appropedia.org/CNC_Router_Parts_metal_3D_printer.

[54] Haselhuhn, Amberlee S., et al. “In Situ Formation of Substrate Release Mechanisms for Gas Metal Arc Weld Metal 3-D Printing.” *Journal of Materials Processing Technology*, vol. 226, Dec. 2015, pp. 50–59., doi:10.1016/j.jmatprotec.2015.06.038.

[55] Haselhuhn, Amberlee S., et al. “Hypoeutectic Aluminum–Silicon Alloy Development for GMAW-Based 3-D Printing Using Wedge Castings.” *International Journal of Metalcasting*, vol. 11, no. 4, 25 Jan. 2017, pp. 843–856., doi:10.1007/s40962-017-0133-z.

[56] IvánTabernero, et al. “Study on Arc Welding Processes for High Deposition Rate Additive Manufacturing.” *Procedia CIRP*, vol. 68, 23 Apr. 2018, pp. 358–362., doi:10.1016/j.procir.2017.12.095.

[57] "Metal Printing Tool Add-on for Any CNC Machine." *YouTube*, YouTube, 21 Sept. 2018, www.youtube.com/watch?v=sda0Z9j2SbI.

[58] Blue Demon Welding Products, "AL 5356 Aluminum Mig Welding Wire," Datasheet, N.D. https://www.globalweldingsupplies.co.nz/upload/PDF/Datasheet_BD_ER5356_V1.pdf [Accessed: Mar. 4, 2021]

[59] "Aluminum 5356 Alloy (UNS A95356)." *AZoM.com*, 11 July 2013, www.azom.com/article.aspx?ArticleID=6654.

[60] The Harris Product Group., "5356 Aluminum Weld Wire," Datasheet, N.D.

[61] Haselhuhn, Amberlee. "Aluminum Substrate Cleaning for 3-D Printing:MOST." *Appropedia*, 24 Mar. 2016, www.appropedia.org/Aluminum_substrate_cleaning_for_3-D_printing:MOST.

[62] Miao, Qiuyu, et al. "Comparative Study of Microstructure Evaluation and Mechanical Properties of 4043 Aluminum Alloy Fabricated by Wire-Based Additive Manufacturing." *Materials & Design*, vol. 186, 15 Jan. 2020, p. 108205., doi:10.1016/j.matdes.2019.108205.

[63] *Hobart SpoolRunner 100*. Hobart Welding Products., Troy., OH, USA, 2012.

[64] "Our Fastest CT System Delivered to Boeing." *X-Ray Equipment*, 4nsi.com/news/2014/03/25/ct-system-delivered-to-boeing/.

[65] *Nano 2000T Polisher*. Pace Technologies., Tucson., AZ, USA, March 8, 2016, pp. 1. https://www.metallographic.com/Brochures/NANO-2000T-Instruction-Manual.pdf

[66] "Digital Microscope." *KEYENCE*, www.keyence.com.sg/products/microscope/digital-microscope/vhx-900/.

[67] *IronMan 230 And M-25 Gun.* Hobart Welding Products., Appleton., WI, USA, 2018, pp. 23.

[68] "Etchant Database." *Pace Technology - Etchant Database*, database.metallographic.com/pace-etchant.php.

[69] ASTM International. *E407-07(2015)e1 Standard Practice for Microetching Metals and Alloys*. West Conshohocken, PA; ASTM International, 2015. doi: https://doi.org/10.1520/E0407-07R15E01

[70] "Color 3D Laser Microscope." *KEYENCE*, www.keyence.com/products/microscope/laser-microscope/vk-8700_9700_generationii/models/vk-9710k/.

[71] ASTM International. E8/E8M-21 Standard Test Methods for Tension Testing of Metallic Materials. West Conshohocken, PA; ASTM International, 2021. doi: https://doi.org/10.1520/E0008_E0008M-21

[72] ASTM International. *B557M-15 Standard Test Methods for Tension Testing Wrought and Cast Aluminum- and Magnesium-Alloy Products (Metric)*. West

Conshohocken, PA; ASTM International, 2015.
doi: https://doi.org/10.1520/B0557M-15

[73] "Get the Facts on... Porosity in Metal Additive Manufacturing." *Get the Facts on... Porosity in Metal Additive Manufacturing | GE Additive*, GE Additive, 10 Mar. 2021, www.ge.com/additive/blog/get-facts-porosity-metal-additive-manufacturing#:~:text=Porosity%20is%20often%20thought%20to,the%20properties%20of%20the%20part.

[74] Slotwinski, John A., et al. "Porosity Measurements and Analysis for Metal Additive Manufacturing Process Control." *Journal of Research of the National Institute of Standards and Technology*, vol. 119, 16 Sept. 2014, doi:10.6028/jres.119.019.

[75] Kamoon, B., Dahe, S.A., & Obaid, Z.H. (2020). Microstructural Evaluation for TIG Welding of AA6061-T6 using ER5356 Filler Metal; in Postweld and as-Weld Treatment.

[76] Kaufman, J. G. (Ed.). (1999). Properties of aluminum alloys: Tensile, creep, and fatigue data at high and low temperatures. ASM International.

[77] Stratasys Direct Manufacturing. *Aluminum AlSi10Mg: Direct Metal Laser Melting Material Specification*, 2015, info.stratasysdirect.com/rs/626-SBR-192/images/DMLM_Aluminum_AlSi10Mg_Material_Datasheet_202002.pdf.

[78] *Aluminum GMAW: Gas Metal Arc Welding for Aluminum Guide.* Lincoln Welding., Cleveland., OH, January 2016, pp. 21

[79] Haselhuhn, Amberlee S, Buhr, Michael W, Wijnen, Bas, Sanders, Paul G, & Pearce, Joshua M. (2016). Structure-property relationships of common aluminum weld alloys utilized as feedstock for GMAW-based 3-D metal printing. *Materials Science & Engineering. A, Structural Materials: Properties, Microstructure and Processing*, *673*, 511–523. https://doi.org/10.1016/j.msea.2016.07.099

[80] "Common Design Mistakes in Aluminum: Lincoln Electric." *Lincolnelectric*, www.lincolnelectric.com/en-us/support/welding-how-to/Pages/aluminum-design-mistakes-detail.aspx.

APPENDIX

Part Name	Cost	Source	Part Number	Quantity	Link	Total Part Cost	Misc Info
HIWIN Rail Assembly (1 carriage, 1000mm)	112	HIWIN	HGW-20-CC-1R1000-Z0-C	6	https://motioncontrolsystems.h	672	4 rails in the z axis, 2 rails in the y axis
HIWIN Rail Assembly (2 carriage, 1200mm)	159	HIWIN	HGW-20-CC-2R1200-Z0-C	4	https://motioncontrolsystems.h	636	4 rails in the x axis with 2 carriages each to prevent moments of the blocks
Nema 34 Stepper Motors	63.72	StepperOnline	34HS46-5004D	5	https://www.omc-stepperonline	318.6	
Nema 34 Stepper Motor Mount	9.99	Amazon	N/A	5	https://www.amazon.com/Step	49.95	
BallScrew Assembly - 1.5 m	311.64	Automation4Less	BSFU2005-1500-FS	2	http://www.automation4less.co	623.28	Fixed End: BK15; Floating End: BF15; Ball Nut Bracket: Aluminum
BallScrew Assembly - 1 m	267.64	Automation4Less	BSFU2005-1000-FS	1	http://www.automation4less.co	267.64	Fixed End: BK15; Floating End: BF15; Ball Nut Bracket: Aluminum
Milling Spindle - 2.2 kW Water Cooled Spindle with Inverter (VFD) (220V)	528	BuildyourCNC	N/A	1	https://buildyourcnc.com/item/	528	220 option
Mega 2560 R3 Mega2560 REV3 + 1pcs RAMPS 1.4 Controller for 3D arduino kit Reprap MendelPrusa	13.75	Newegg	MW	1	https://www.newegg.com/Prod	13.75	Price may change with sale
relay	5.98	amazon	3-01-0340	1	https://www.amazon.com/HiLet	5.98	
Digital Stepper Driver 1.8~5.6A 20-50VDC for Nema 23, 24, 34 Stepper Motor	35.64	StepperOnline	DM556T	5	https://www.omc-stepperonline	178.2	ordering all 5 at once will give us a quantity discount
push button red e-stop + 6 end stop swithes	13.55	amazon	619191020638	1	https://www.amazon.com/Butto	13.55	
worm gear box	57	Amazon	RV030-80-nema23	1	https://www.amazon.com/Gear	57	
dual shaft nema 17	14.97	StepperOnline	17HS24-2104D	1	https://www.omc-stepperonline	14.97	
Nema 23 CNC Stepper Motor	39.99	amazon/stepper onlin	FBA_23HS45-4204S	1	https://www.amazon.com/Torq	39.99	
stepper driver (nema 23)	15.69	amazon	TB6600 4A	2	https://www.amazon.com/Step	31.38	
ACME Screw Assembly - 3/4	565	Helix Linear	075-RA/3L/4N/39.00/2007	2	https://www.helixlinear.com/m	1130	Quote Attached
C-Channel C8x11.5	87.23	Midwest Steel	72 inches long	2	https://www.midweststeelsupp	174.46	Does not need to come from midwest steel. Anywhere will work
C-Channel C8x11.5	64.71	Midwest Steel	50 inches long	3	https://www.midweststeelsupp	194.13	
24V 20A 500W Power Supply AC 100-240V Input	29.73	Amazon	B077N592WJ	2	https://www.amazon.com/Switc	59.46	
12V 50A power supply	55.98	amazon	LT-PS12V-50A	1	https://www.amazon.com/96V-	55.98	
12V 30A power supply	23.99	amazom	SQUEEVI19514	1	https://www.amazon.com/ALITC	23.99	
5V power supply	13.99	amazon	8541605486	1	https://www.amazon.com/PHEV	13.99	
Leveling Feet	79.99	Amazon	N/A	1	https://www.amazon.com/Caste	79.99	
Hobart IronMan 230 Flux-Cored/MIG Welder with Spool Gun and Cart	1649.99	Tractor Supply Co	Model# 500536001	1	https://www.tractorsupply.com/	1649.99	
Hobart Spool Gun	559	Northern Tool	300349	1	https://www.northerntool.com/	559	if possible pickup in Sioux Falls
Aluminum Spools	10.34	Amazon	N/A	25	https://www.amazon.com/Blue-	258.5	
HIWIN Carriages	127.59	McMaster	6709K13	2	https://www.mcmaster.com/67	255.18	flanged, for 20 mm rail, 30mmx63mmx74mm dimensions
BarbFitting G1/4 Thread Barb Connector for	4.59	Amazon		1	https://www.amazon.com/Bewi	4.59	
Hose Clamp	5.98	Amazon		1	https://www.amazon.com/Preci	5.98	
Flexible High Pressure, Reinforced, Vinyl Tubing(1/4" ID x 3/8" OD x	24.99	Amazon		1	https://www.amazon.com/Hydr	24.99	
3-Pack Fan 120mm Cooling Fan	11.99	Amazon		1	https://www.amazon.com/uphe	11.99	
Radiator Water Cooler Heat Sink 360mm	33.99	Amazon		1	https://www.amazon.com/Com	33.99	
100ft - 1 inch Flexo PET Expandable Braided Sleeving – Black – Alex Tech Braided Cable Sleeve	18.99	Amazon	N/A	1	https://www.amazon.com/dp/B	18.99	
.190 Aluminum sheet 3'x3'	71.71	Midwest Steel		1	https://www.midweststeelsupp	71.71	
.125 Aluminum sheet 3'x3'	86.7	Midwest Steel		1	https://www.midweststeelsupp	86.7	
.063 Aluminum sheet 3'x3'	64.76	Midwest Steel		1	https://www.midweststeelsupp	64.76	
250ft 14awg 4 connector wire	46.95	amazon	4330098827	1	https://www.amazon.com/250ft	46.95	
4pin automotive wire connectors	4.31	ebay		30	https://www.ebay.com/itm/6-3	129.3	
22awg solid jumper wire	14.99	amazon		1	https://www.amazon.com/TUOF	14.99	
pin connectors	6.98	amazon		1	https://www.amazon.com/Gikfu	6.98	
head connector housing	9.5	amazon		1	https://www.amazon.com/CynK	9.5	
25mm x 103mm Plastic Wire Carrier 1M Length R55	34.99	Amazon		2	https://www.amazon.com/uxcel	69.98	
Black Plastic Drag Chain Cable Carrier 10 x 15mm	9.39	Amazon		1	https://www.amazon.com/uxcel	9.39	
					total	8515.75	